



Cite this: DOI: 10.1039/c6dt04094b

Coordination of bis(azol-1-yl)methane-based bisphosphines towards Ru^{II}, Rh^I, Pd^{II} and Pt^{II}: synthesis, structural and catalytic studies†

Sajad A. Bhat,^a Madhusudan K. Pandey,^a Joel T. Mague^b and Maravanji S. Balakrishna^{*a}

The coordination chemistry of bisphosphine ligands assembled on the five-membered heterocyclic platform of bis(azol-1-yl)methane *viz.*: bis(2-diphenylphosphinoimidazol-1-yl)methane (**1**), bis(5-diphenylphosphinopyrazol-1-yl)methane (**2**) and bis(5-diphenylphosphino-1,2,4-triazol-1-yl)methane (**3**) with Ru^{II}, Rh^I, Pd^{II} and Pt^{II} is described. The bisphosphines **1–3** react with elemental selenium to give the corresponding bis-selenoyl derivatives **4–6**. The reactions of **1–3** with transition metal derivatives produce complexes with different coordination modes. Bisphosphine **1** showed a preference for the κ^2 -*P,P* mode of coordination, whereas bisphosphines **2** and **3**, besides the κ^2 -*P,P* mode also showed a head-to-tail κ^2 -*P,N* coordination mode resulting in the formation of binuclear complexes [Rh₂(COD)₂((CH₂(1,2-C₃H₂N₂PPh₂)₂)- κ^2 -*P,N*)] [BF₄]₂ (**14**), [Rh₂(COD)₂((CH₂(1,2,4-C₂H₃N₃PPh₂)₂)- κ^2 -*P,N*)] [BF₄]₂ (**15**), [Pd₂(η³-C₃H₅)₂((CH₂(1,2-C₃H₂N₂PPh₂)₂)- κ^2 -*P,N*)] [BF₄]₂ (**21**) and [Pd₂(η³-C₃H₅)₂((CH₂(1,2,4-C₂H₃N₃PPh₂)₂)- κ^2 -*P,N*)] [BF₄]₂ (**22**). Several of these complexes have also been structurally characterized. The *in situ* generated Rh^I complex of bisphosphine **1** showed moderate to good selectivity in the hydroformylation of various styrene derivatives.

Received 25th October 2016,
Accepted 23rd November 2016
DOI: 10.1039/c6dt04094b

www.rsc.org/dalton

Introduction

Despite a plethora of phosphorus based ligands available,¹ the enthusiasm to generate new ones or to carry out structural modifications of the existing ones is essentially due to the overwhelming demand for modulating the reactivity of metal complexes with relevance to their applications in homogeneous catalysis. Due to the readily available steric and electronic characteristics and the ability to provide well-defined and desired coordination environments around metal centers, bisphosphines are the most preferred ligands in homogeneous catalysis and other important applications.² A variety of bisphosphine ligands with varied bite angles have been synthesized and their coordination chemistry has been explored.³

Mixed donor ligands or phosphines containing nitrogen heterocycles as substituents are also of importance in coordination chemistry.⁴ The presence of a hetero donor atom gives flexible coordination modes and also facilitates the dis-

sociation of at least one of the metal–ligand bonds with a smaller kinetic barrier simply due to the difference in the Lewis acid–base compatibilities. Among phosphines and nitrogen-heterocycle-based hybrid systems, more attention has been devoted to the phosphine–pyridine and the phosphine–imidazole ligands and only a limited number of complexes containing phosphine–pyrazole or phosphine-1,2,3/4-triazole have been reported.⁵ The phosphine–imidazole ligands have been used in the synthesis of various mono- and bi-metallic complexes⁷ and also in several organic transformations.⁶ Otero *et al.* have reported the first examples of bis(azol-1-yl)methane-based bisphosphines *viz.* bis(2-diphenylphosphinoimidazol-1-yl)methane (bpizm) and bis(5-diphenylphosphinopyrazol-1-yl)methane (bppzm) and studied the coordination chemistry of a bppzm ligand with Nb^{III}, Pd^{II} and Pt^{II} metal centres.^{8a,b} In recent years, Chauvin and co-workers have synthesized *o/m*-phenylene bridged bis(imidazolylphosphines) and studied their *cis/trans* chelating behaviour towards Rh^I and Pd^{II} metal centres.⁹ As a continuation of our work in designing new phosphorus based ligands with a flexible P...P bite for exploring their organometallic chemistry and catalytic applications,¹⁰ we decided to contribute to the so far unexplored chemistry of bisphosphines based on bis(azol-1-yl)methane by preparing a new member of this family, bis(5-diphenylphosphino-1,2,4-triazol-1-yl)methane, and to investigate its transition metal chemistry. For comparison, the coordination chemistry of

^aPhosphorus Laboratory, Department of Chemistry, Indian Institute of Technology Bombay, Powai, Mumbai, 400076, India. E-mail: krishna@chem.iitb.ac.in, msb_krishna@iitb.ac.in

^bDepartment of Chemistry, Tulane University, New Orleans, Louisiana, 70118, USA

† Electronic supplementary information (ESI) available. CCDC 1408417, 1408420, 1511155–1511163, 1517753 and 1517754. For ESI and crystallographic data in CIF or other electronic format see DOI: 10.1039/c6dt04094b

bisphosphines such as bis(2-diphenylphosphinoimidazol-1-yl)methane and bis(5-diphenylphosphinopyrazol-1-yl)methane was also undertaken.

Results and discussion

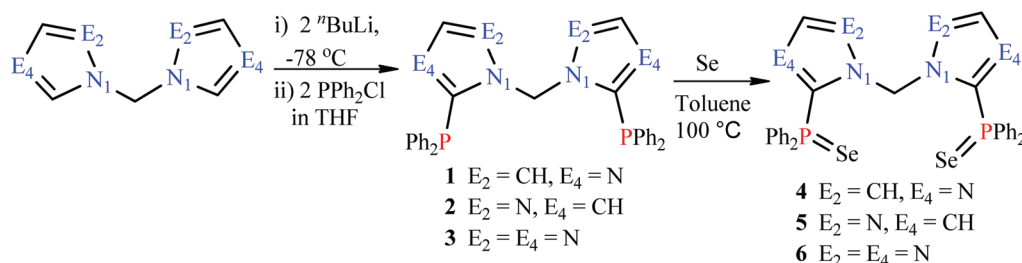
Bisphosphine ligands **1–3** were synthesized according to the reported literature procedures.^{8a,c} The lithiated salts of bis(azol-1-yl)methanes (azole, imidazole, pyrazole, 1,2,4-triazole) were generated by treatment with two equivalents of ⁿBuLi in tetrahydrofuran at $-78\text{ }^{\circ}\text{C}$, which on further reaction with two equivalents of chlorodiphenylphosphine resulted in the formation of desired bisphosphines as shown in Scheme 1. The $^{31}\text{P}\{^1\text{H}\}$ NMR spectra of **1–3** showed single resonances around -34.5 ppm . In order to quantify the σ -donor properties of bisphosphines **1–3**, selenoyl derivatives **4–6** were synthesized by treating **1–3** with an excess of elemental selenium powder in toluene at $100\text{ }^{\circ}\text{C}$.

The $^{31}\text{P}\{^1\text{H}\}$ NMR spectra of compounds **4–6** showed singlets at 17.8, 15.7 and 17.9 ppm with $^1J_{\text{PSe}}$ couplings of 729, 746 and 754 Hz, respectively. Usually the electron withdrawing groups on phosphorus increase the magnitude of phosphorus–selenium coupling constant ($^1J_{\text{PSe}}$), due to the increased *s*-character of the phosphorus orbital involved in P–Se bonding and *vice versa*.^{11a} The magnitude of $^1J_{\text{PSe}}$ for **6** suggests a slightly more *s*-character and hence a marginally

weaker σ -donor ability compared to that of compounds **4**, **5** and PPh_3 ($^1J_{\text{PSe}} = 730\text{ Hz}$).¹¹ In the ^1H NMR spectra of **4–6**, the bridging methylene protons did not show $^4J_{\text{PH}}$ coupling, whereas the parent compounds **1–3** showed the same in the range of 1.5–2 Hz.

The structures of **1**, **2** and **4–6** were confirmed by single crystal X-ray diffraction studies. The perspective views of the molecular structures of **1** and **2** along with selected bond distances and bond angles are shown in Fig. 1. Due to the free rotation about the N–C_{sp³}–N unit in both **1** and **2**, the two azole rings are not coplanar. Since the two phosphorus atoms in **2** are in the *syn* conformation with respect to the bis(pyrazol-1-yl)methane bridge, the P...P separation (P1...P2, 4.002 Å) is shorter than that in **1** (5.476 Å, the two phosphorus atoms are in the *anti*-position) and bis(2-(diphenylphosphino)phenyl)ether (4.876 Å),^{12a} but longer compared to those of the short bite ligands such as bis(diphenylphosphino)benzene (3.194 Å) and 2,3-bis(diphenylphosphino)quinoxaline (3.166 Å).^{12b} The intramolecular N1...N4 separation in **2** is 3.298 Å. The P–C bond distances and C–P–C bond angles in **1** and **2** compare well with those reported for analogous phosphine ligands.^{9c}

All the three bis-selenides **4–6** have been structurally characterized. Crystals were obtained from dichloromethane–petroleum ether mixtures. The phosphorus atoms are in a typical tetrahedral environment in all the cases (Fig. 2). The P–C and



Scheme 1 Synthesis of ligands **1–3** and their selenoyl derivatives **4–6**.

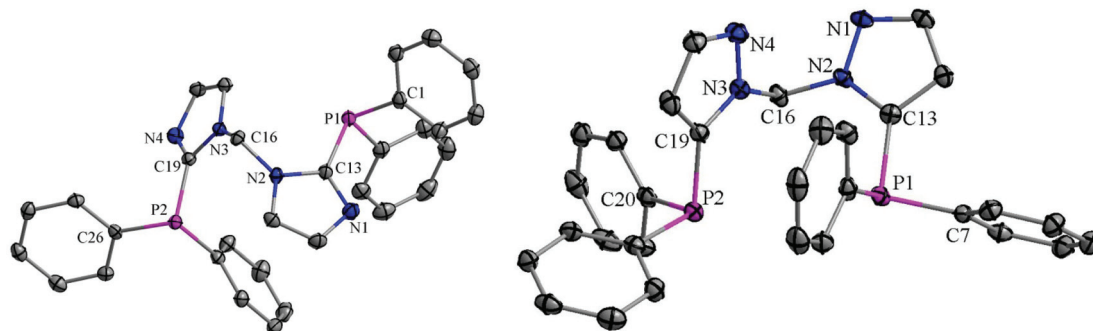


Fig. 1 Molecular structures of $[\text{CH}_2(1,3\text{-C}_3\text{H}_2\text{N}_2\text{PPh}_2)_2]$ (**1**) and $[\text{CH}_2(1,2\text{-C}_3\text{H}_2\text{N}_2\text{PPh}_2)_2]$ (**2**). Thermal ellipsoids are drawn at 50% probability level. Hydrogen atoms have been omitted for clarity. Selected bond lengths (Å) and bond angles ($^{\circ}$): bisphosphine **1**: P1–C13 1.8219(17), P2–C19 1.8206(15), P1–C1 1.8279(17), P1–C7 1.8339(17), P2–C20 1.8335(15), P2–C26 1.8314(15), C1–P1–C7 102.55(8), C1–P1–C13 99.85(8), C7–P1–C13 100.18(8), P1–C13–N1 127.25(13), P1–C13–N2 122.05(12). Bisphosphine **2**: P1–C13 1.8212(15), P2–C19 1.8255(15), P1–C1 1.8349(16), P1–C7 1.8366(18), P2–C20 1.8360(2), P2–C26 1.8345(14), C1–P1–C7 102.49(8).

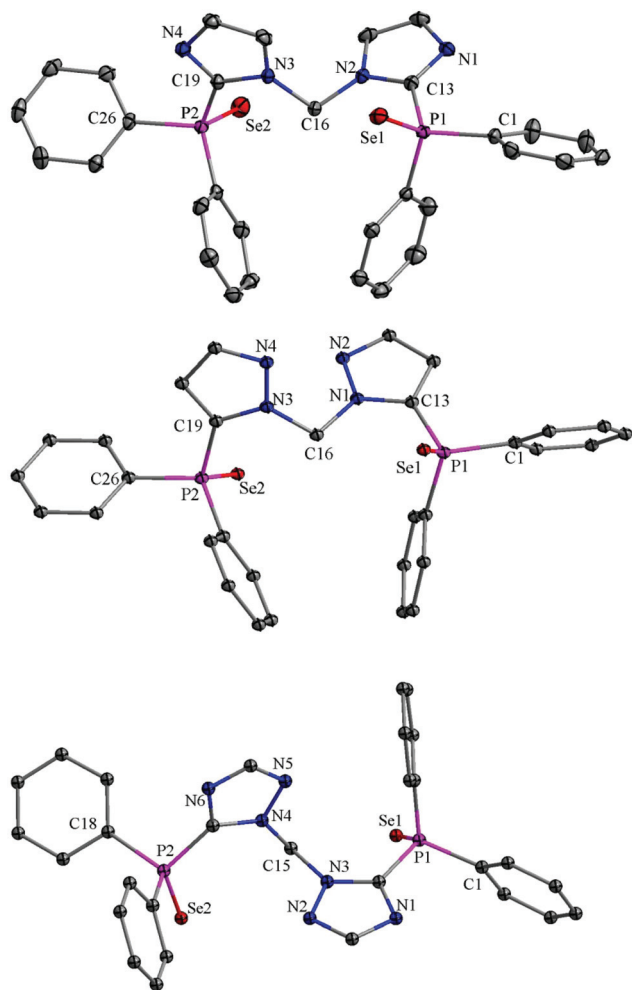


Fig. 2 Molecular structures of $[\text{CH}_2(1,3\text{-C}_3\text{H}_2\text{N}_2\text{PPh}_2\text{Se})_2]$ (**4**), $[\text{CH}_2(1,2\text{-C}_3\text{H}_2\text{N}_2\text{PPh}_2\text{Se})_2]$ (**5**) and $[\text{CH}_2(1,2,4\text{-C}_2\text{HN}_3\text{PPh}_2\text{Se})_2]$ (**6**). Thermal ellipsoids are drawn at 50% probability level. Hydrogen atoms have been omitted for clarity. Selected bond lengths (Å) and bond angles (°) for compound **4**: P1–Se1 2.1043(6), P2–Se2 2.1066(7), P1–C13 1.8145(17), P2–C19 1.8127(18). Compound **5**: P1–Se1 2.1059(8), P2–Se2 2.1064(8), P1–C13 1.803(3), P2–C19 1.802(3). Compound **6**: P1–Se1 2.102(3), P2–Se2 2.091(3), P1–C13 1.813(8), P2–C17 1.811(9).

P–Se bond lengths are consistent with covalent radii predictions as well as typical bond lengths for related diaryl phosphine selenides.¹³ The P–Se bond distances in **4** [2.1043(6) Å, 2.1066(7) Å], **5** [2.1059(8) Å, 2.1064(8) Å] and **6** [2.102(3) Å, 2.091(3) Å] show marginal variations. The intramolecular P...P distances in **4–6** [6.472 Å, 6.320 Å, 6.866 Å] are longer than those found in the parent bisphosphine ligands **1** and **2** [4.002 Å, and 5.476 Å respectively].

Synthesis of Ru^{II}, Rh^I, Pd^{II} and Pt^{II} complexes

The exocyclic phosphine arms appended to the nitrogen heterocycles in **1–3** can move around easily due to the free rotation around the methylene bridge and therefore will influence their ability to achieve chelating or bridging modes of coordination. They offer several coordination possibilities as

shown in Chart 1. Although, chelating and bridging modes are the most preferred coordination modes for soft and low-valent metals, with hard metals such as Nb^{III}, examples of complexes adopting bridging mode **IV** have been reported by Otero and co-workers.^{8a,b} Recently, we have examined the coordination behaviour of ligands **1** and **3** with group 11 metals.^{8c,14} In the case of gold(i) derivatives, besides gold atom showing linear geometry, complexes with trigonal and tetrahedral geometries were also isolated and structurally characterized. In this context, we considered studying the platinum group chemistry owing to their catalytic potential in various organic reactions.

Equimolar reactions between ligands **1–3** and $[\text{RuCl}_2(\eta^6\text{-}p\text{-cymene})]_2$ in dichloromethane at room temperature resulted in the formation of dinuclear complexes $[\text{Ru}_2\text{Cl}_4(\eta^6\text{-}p\text{-cymene})_2\{(\text{CH}_2(1,3\text{-C}_3\text{H}_2\text{N}_2\text{PPh}_2)_2)\text{-}\kappa^2\text{P,P}\}]$ (**7**), $[\text{Ru}_2\text{Cl}_4(\eta^6\text{-}p\text{-cymene})_2\{(\text{CH}_2(1,2\text{-C}_3\text{H}_2\text{N}_2\text{PPh}_2)_2)\text{-}\kappa^2\text{P,P}\}]$ (**8**) and $[\text{Ru}_2\text{Cl}_4(\eta^6\text{-}p\text{-cymene})_2\{(\text{CH}_2(1,2,4\text{-C}_2\text{HN}_3\text{PPh}_2)_2)\text{-}\kappa^2\text{P,P}\}]$ (**9**) as brick red solids with the bisphosphines exhibiting bridged coordination modes as shown in Scheme 2. The $^{31}\text{P}\{^1\text{H}\}$ NMR spectra of **7–9** showed single resonances at 11.3, 15.8 and 13.7 ppm, respectively. The ^1H NMR spectra of complexes **7** and **9** consists of two sets of doublets for the methyl protons of the isopropyl groups at 0.98, 1.01 and 1.17, 1.20 ppm with a $^3J_{\text{HH}}$ coupling of 6.9 Hz and septets at 2.60 and 2.85 ppm for the methine proton $[\text{CH}(\text{Me})_2]$. Two sets of doublets are observed for the *p*-cymene ring protons of **7** and **9** in the range of 5.09–5.31 ppm and 4.89–5.59 ppm, respectively. Similar observations are reported for the analogous Ru^{II} complexes containing cymene groups due to the different orientations of the cymene rings.¹⁵ In complex **8**, two doublets at 5.81 and 4.71 ppm are observed for the *p*-cymene ring protons, whereas two sets of doublets are observed at 1.41 and 1.32 ppm for the methyl protons of the isopropyl group.

The reactions of **1–3** with $[(\eta^5\text{-C}_5\text{H}_5)\text{RuCl}(\text{PPh}_3)_2]$ in 1:1 ratios in toluene under refluxing conditions afforded mononuclear complexes $[(\eta^5\text{-C}_5\text{H}_5)\text{RuCl}\{(\text{CH}_2(1,3\text{-C}_3\text{H}_2\text{N}_2\text{PPh}_2)_2)\text{-}\kappa^2\text{P,P}\}]$ (**10**), $[(\eta^5\text{-C}_5\text{H}_5)\text{RuCl}\{(\text{CH}_2(1,2\text{-C}_3\text{H}_2\text{N}_2\text{PPh}_2)_2)\text{-}\kappa^2\text{P,P}\}]$ (**11**) and $[(\eta^5\text{-C}_5\text{H}_5)\text{RuCl}\{(\text{CH}_2(1,2,4\text{-C}_2\text{HN}_3\text{PPh}_2)_2)\text{-}\kappa^2\text{P,P}\}]$ (**12**) as shown in Scheme 2.

The $^{31}\text{P}\{^1\text{H}\}$ NMR spectra of complexes **10–12** showed single resonances at 41.2, 36.7 and 42.5 ppm, respectively. The cyclopentadienyl ring protons in the ^1H NMR spectrum appear in the range 4.10–4.32 ppm. Furthermore, the ^1H NMR spectra of complexes **10–12** showed clearly differentiated *exo* and *endo* protons of the bridging methylene group (CH_2), as they become diastereotopic on complexation. The *endo* proton in **7–9** appears as a doublet at 7.13, 7.08 and 7.18 ppm, respectively, due to the geminal $^2J_{\text{HH}}$ coupling of 14.4 Hz. The *exo* proton also appeared as a doublet at 5.24, 5.99 and 5.99 ppm, respectively, with $^2J_{\text{HH}}$ coupling of 14.4 Hz. The cross peak analysis of the CH_2 protons in the $^1\text{H}\text{-}^1\text{H}$ COSY spectrum of **12** reveals the possible explanation for the observed multiplicity. The $^1\text{H}\text{-}^1\text{H}$ COSY spectrum indicates that the doublet at 5.99 ppm due to one of the CH_2 protons is correlated to the doublet of another proton at 7.18 ppm. This difference in chemical shifts between the pair of doublets arising from the

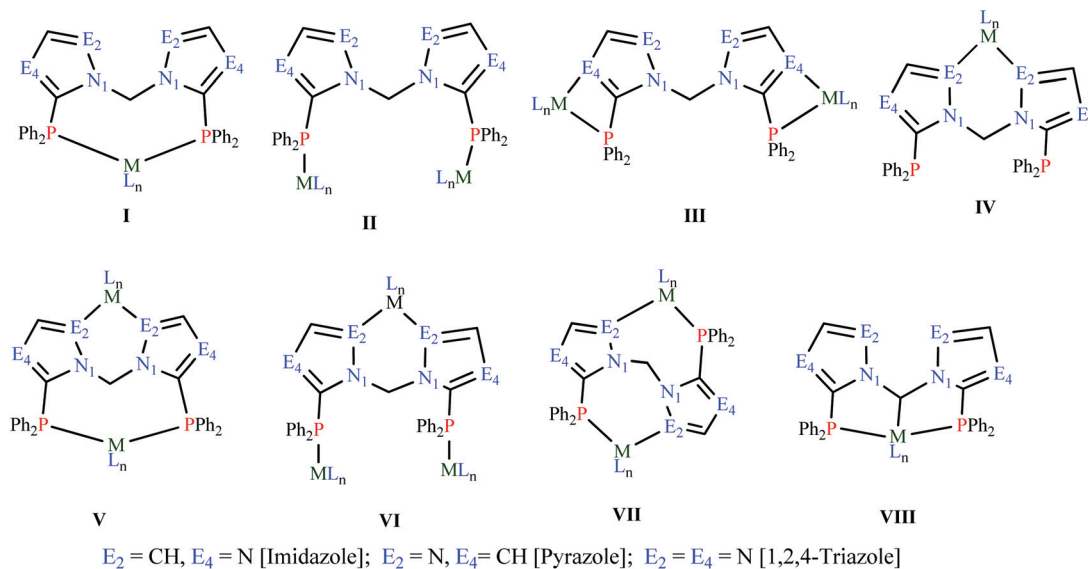
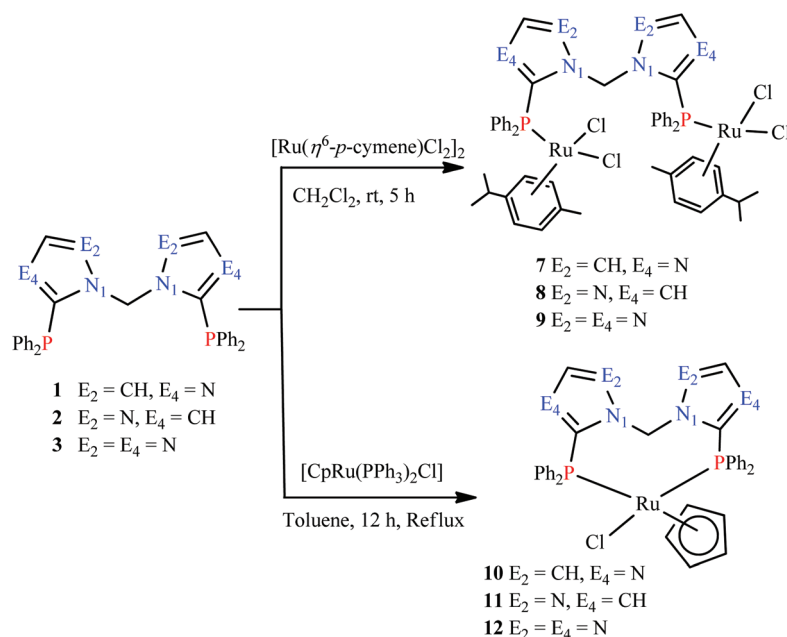


Chart 1 Possible coordination modes for ligands 1–3.



Scheme 2 Synthesis of ruthenium(II) complexes.

–CH₂– moiety in the complexed form of these ligands is particularly sensitive to the nature of the metal precursor, coordination number and the presence of other ligands.

Crystals of complexes **10** and **12** suitable for the single crystal X-ray diffraction study were obtained by slow diffusion of petroleum ether into the dichloromethane solution of the corresponding complex, whereas those of **11** were obtained by slow diffusion of petroleum ether into the chloroform solution. These complexes (**10–12**) have similar bond parameters (Table 1). As revealed from the crystal structures of **10–12** (Fig. 3), ruthenium adopts three-legged *piano stool* geometry

and the conformation of the metallacycle is such that the *endo* proton is in the range of (2.464–2.638 Å) from the chloride atom, whereas the *exo* proton shows CH $\cdots\pi$ interaction (CH_{21A} \cdots C9 = 2.848 Å) with a phenyl ring of another molecule in complex **10**. The P1–Ru–P2, P1–Ru–Cl and P2–Ru–Cl bond angles are in the range of 95.33(3)–96.43(3)°, 87.694(17)–89.12(3)° and 93.536(16)°–100.75(2)°, respectively. The Ru–P bond distances are in the range of 2.2794(6)–2.3060(8) Å and are comparable to the imidazole–phosphine based complex [(η^5 -C₅H₅)RuCl(PPh₃)(C₃N₂H₃PPh₂)] [2.307(1) Å],¹⁶ but are shorter than those observed for [(η^5 -C₅H₅)RuCl{Ph₂PC₆H₄OC₆H₄PPh₂–

Table 1 Selected bond distances and bond angles for **10**, **11** and **12**

	10	11	12
Bond distances (Å)			
Ru1–Cl1	2.4405	2.4581(8)	2.4426(6)
Ru1–P1	2.2859(5)	2.2919(8)	2.2794(6)
Ru1–P2	2.2962(5)	2.3060(8)	2.2924(6)
Ru1–C1	2.196(2)	2.228(3)	2.215(2)
Ru1–C2	2.188(2)	2.223(3)	2.209(2)
Ru1–C3	2.224(2)	2.189(3)	2.181(2)
Ru1–C4	2.222(2)	2.197(3)	2.198(2)
Ru1–C5	2.216(2)	2.220(3)	2.218(2)
Bond angles (°)			
Cl1–Ru1–P1	90.69(2)	89.12(3)	87.79(2)
Cl1–Ru1–P2	93.54(2)	100.43(3)	100.75(2)
P1–Ru1–P2	96.38(2)	95.33(3)	96.43(2)
P1–Ru1–C1	92.06(6)	140.93(10)	142.55(7)
P2–Ru1–C2	96.26(6)	92.83(10)	90.78(7)
P2–Ru1–C3	92.32(6)	94.02(10)	94.21(7)
Cl1–Ru1–C4	89.35(5)	131.63(10)	130.02(7)
P1–Ru1–C5	105.20(6)	104.32(10)	105.88(7)

κ^2P,P].¹⁵ The Ru–C bond distances range from 2.181(2) Å to 2.228(3) Å, in which Ru–C bonds *trans* to phosphine are longer than those *trans* to the chlorine atoms.

The 2 : 1 reaction between **1** and [Rh(COD)Cl]₂ in the presence of two equivalents of AgBF₄ in tetrahydrofuran afforded the cationic chelate complex, [Rh(COD){CH₂(1,3-C₃H₂N₂PPh₂)₂}- κ^2P,P][BF₄]⁺ (**13**), whereas similar reactions of **2** and **3** in 1 : 1 molar ratios in the presence of two equivalents of AgBF₄ yielded bimetallic P,N-chelated complexes [Rh₂(COD)₂{(CH₂(1,2-C₃H₂N₂PPh₂)₂)- κ^2P,N }]₂[BF₄]₂ (**14**) and [Rh₂(COD)₂{(CH₂(1,2,4-C₂HN₃PPh₂)₂)- κ^2P,N }]₂[BF₄]₂ (**15**), respectively, as shown in Scheme 3. The ³¹P{¹H} NMR spectra of complexes **13**–**15** consists of doublets centred at 3.2, 3.8 and 29 ppm with ¹J_{RhP} couplings of 140, 149 and 168 Hz, respectively. The molecular structure of **14** was further confirmed by a single crystal X-ray diffraction study.

Single crystals of [Rh₂(COD)₂{(CH₂(1,2-C₃H₂N₂PPh₂)₂)- κ^2P,N }]₂[BF₄]₂ (**14**) were grown by layering a dichloromethane solution of the complex with diethyl ether. Complex **14** has crystallographically-imposed 2-fold rotation symmetry with the axis passing through the methylene bridge carbon atom (Fig. 4). The bond parameters are given in Table 2. The rhodium(i) atoms are in a typical square planar environment coordinated by a bridging μ - κ^2P,N ligand and an η^2 -COD ligand to form two seven-membered chelate rings. The Rh–P bond distance [2.3265(10) Å] in **14** is longer than that in the PPh₃ ligated complex, [Rh(acac)(CO)(PPh₃)]¹⁷ [2.2418(9) Å], but is comparable to those for [RhCl(PPh₃)₃]¹⁸ [2.322(4) Å, 2.334(4) Å, 2.214(4) Å] and [Rh(COD)(PPh₃)₂][BF₄]¹⁹ [2.3220(10) Å, 2.3618(1) Å].¹⁹ The Rh–N bond distance of 2.123(3) Å falls between the experimental values reported in the literature for analogous complexes containing P,N-donor ligands.^{20,21} The coordination of N2 also decreases the N1–C16–N1 bond angle from 112.29° (N2–C16–N3; free ligand) to 109.2(4)°. The N2–Rh1–P1 bite angle of 90.25(9)° indicates the formation of strain free seven-membered chelate ring with the rhodium atoms in an ideal

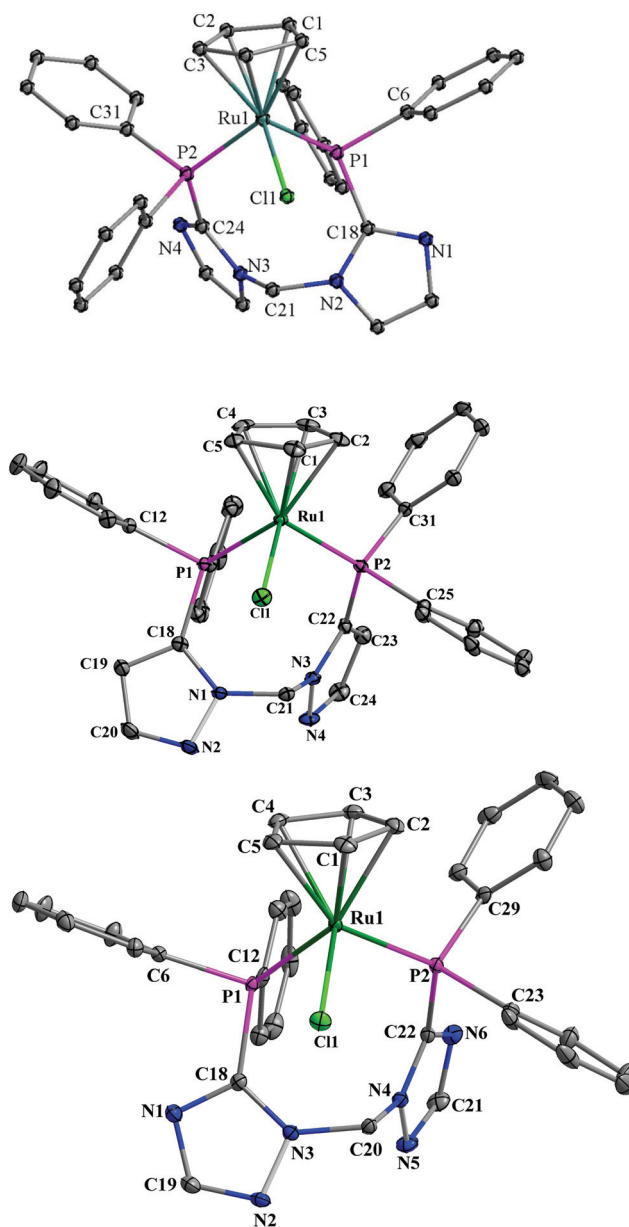
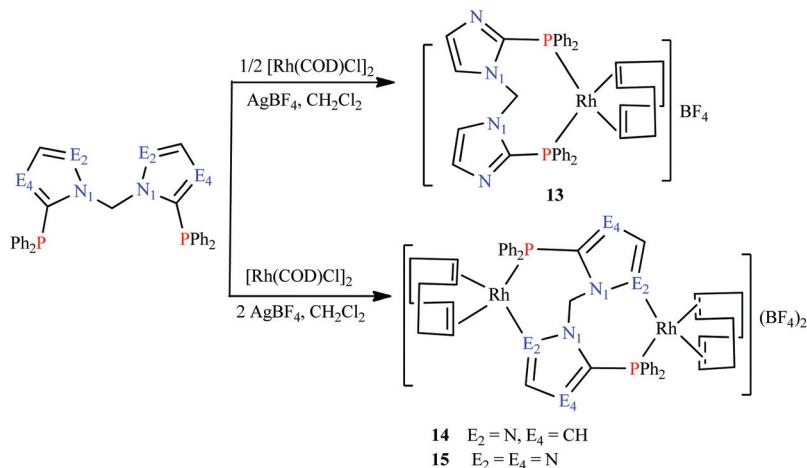


Fig. 3 Molecular structures of [(η^5 -C₅H₅)RuCl{(CH₂(1,3-C₃H₂N₂PPh₂)₂)- κ^2P,P }] (**10**), [(η^5 -C₅H₅)RuCl{(CH₂(1,2-C₃H₂N₂PPh₂)₂)- κ^2P,P }] (**11**) and [(η^5 -C₅H₅)RuCl{(CH₂(1,2,4-C₂HN₃PPh₂)₂)- κ^2P,P }] (**12**). Thermal ellipsoids are drawn at 50% probability level. Hydrogen atoms have been omitted for clarity.

square planar geometry. This bite angle is larger than those reported for analogous six-membered chelate complexes of the type [Rh{3,5-Me₂-C₃HN₂CH₂CH₂PPh₂}- κ^2P,N](COD)][BF₄]²⁰ (82.68(5)°) and [Rh{C₃H₃N₂CH₂CH₂PPh₂}- κ^2P,N](COD)][BF₄]²¹ (88.86(4)°).

The treatment of bisphosphines **1** and **3** with a stoichiometric amount of [M(COD)Cl]₂ (M = Pd, Pt) in dichloromethane at room temperature resulted in the formation of eight-membered chelate complexes [MCl₂{(CH₂(1,3-C₃H₂N₂PPh₂)₂)- κ^2P,P }] (**16** M = Pd, **17** M = Pt) and [MCl₂{(CH₂(1,2,4-C₂HN₃PPh₂)₂)- κ^2P]



Scheme 3 Synthesis of rhodium(I) complexes.

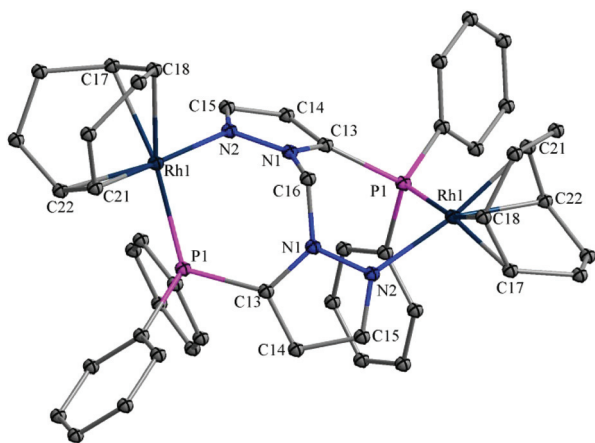


Fig. 4 Molecular structure of $[\text{Rh}_2(\text{COD})_2]\{(\text{CH}_2(1,2\text{-C}_3\text{H}_2\text{N}_2\text{PPh}_2)_2)\text{-}\kappa^2\text{P,N}\}[\text{BF}_4]_2$ (**14**). Thermal ellipsoids are drawn at 50% probability level. Hydrogen atoms have been omitted for clarity.

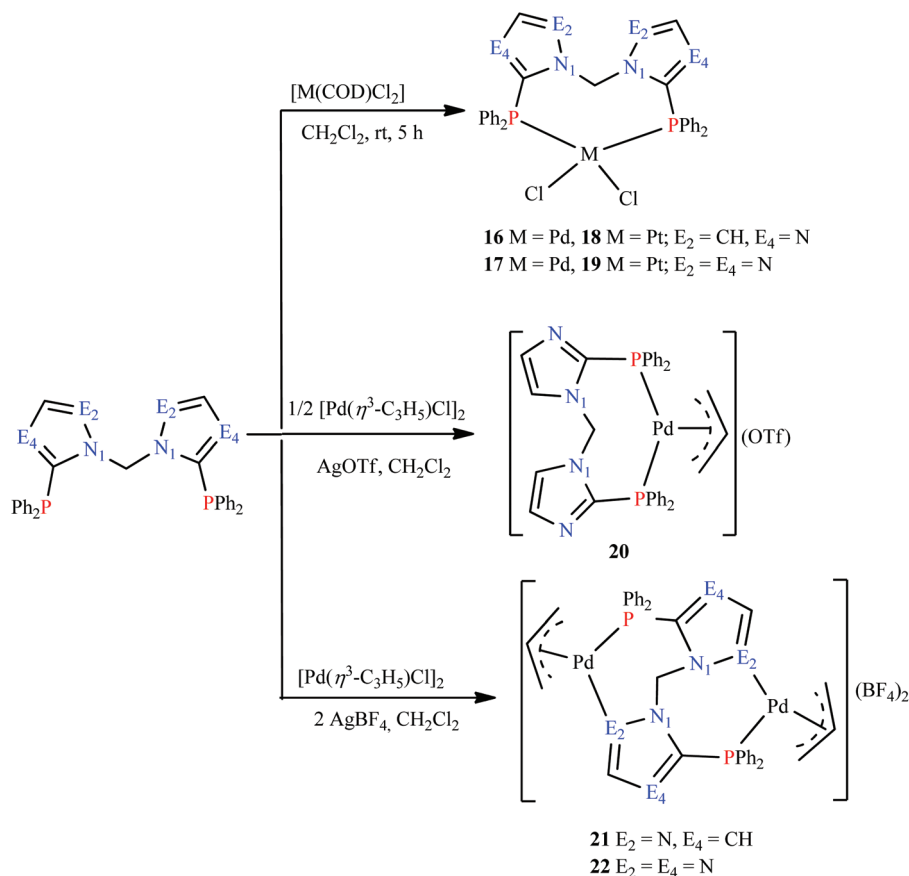
Table 2 Selected bond distances and bond angles for **14**

Bond distances (Å)		Bond angles (°)	
Rh1–P1	2.3265(10)	N2–Rh1–P1	90.25(9)
Rh1–N2	2.123(3)	C22–Rh1–C17	82.32(16)
Rh1–C17	2.229(4)	C21–Rh1–C18	81.23(16)
Rh1–C18	2.202(4)	N2–Rh1–C18	90.76(15)
Rh1–C21	2.148(4)	N2–Rh1–C17	89.75(14)
Rh1–C22	2.126(4)	C22–Rh1–P1	90.84(13)
N1–N2	1.350(5)	C21–Rh1–P1	93.92(12)
N1–C13	1.359(5)	C18–Rh1–P1	159.51(12)
N2–C15	1.338(5)	C21–Rh1–N2	167.47(15)
		N1–C16–N1	109.2(4)

$P\}} (18 \text{ M} = \text{Pd}, 19 \text{ M} = \text{Pt})$ as shown in Scheme 4. The $^{31}\text{P}\{^1\text{H}\}$ NMR spectra of complexes **16–19** showed single resonances at 11.8, 8.1, -9.9 , and -7.4 ppm, with platinum complexes **18** and **19** showing $^1J_{\text{PtP}}$ couplings of 3454 and 3473 Hz, respectively. The larger $^1J_{\text{PtP}}$ coupling supports the *cis*-orientation of phosphorus atoms around the platinum centre.^{22–26}

The cationic complex $[\text{Pd}(\eta^3\text{-C}_3\text{H}_5)\{(\text{CH}_2(1,3\text{-C}_3\text{H}_2\text{N}_2\text{PPh}_2)_2)\text{-}\kappa^2\text{P,P}\}][\text{OTf}]$ (**20**) was prepared by the reaction of **1** with $[\text{Pd}(\eta^3\text{-C}_3\text{H}_5)\text{Cl}]_2$ in a 2 : 1 molar ratio in the presence of AgOTf. The analogous reactions of **2** and **3** with $[\text{Pd}(\eta^3\text{-C}_3\text{H}_5)\text{Cl}]_2$ in 1 : 1 molar ratios in the presence of two equivalents of AgBF₄ in tetrahydrofuran afforded dinuclear complexes $[\text{Pd}_2(\eta^3\text{-C}_3\text{H}_5)_2\{(\text{CH}_2(1,2\text{-C}_3\text{H}_2\text{N}_2\text{PPh}_2)_2)\text{-}\kappa^2\text{P,N}\}][\text{BF}_4]_2$ (**21**) and $[\text{Pd}_2(\eta^3\text{-C}_3\text{H}_5)_2\{(\text{CH}_2(1,2,4\text{-C}_2\text{HN}_3\text{PPh}_2)_2)\text{-}\kappa^2\text{P,N}\}][\text{BF}_4]_2$ (**22**). The $^{31}\text{P}\{^1\text{H}\}$ NMR spectra of **20–22** showed single resonances at 0.01, 8.8 and 11.3 ppm, respectively. The ^1H NMR spectral data are consistent with the structures proposed and the structure of **21** was further confirmed by a single crystal X-ray diffraction study.

The crystals of **16–18** suitable for the X-ray diffraction study were obtained by slow diffusion of diethyl ether into a dichloromethane solution of the corresponding complexes. Selected bond distances and bond angles are listed in Table 3. The bridging CH₂ unit of the ligand is located above the mean plane of the Cl₂MP₂ unit and the dihedral angle (φ) between P1–Pd1–P2 and P1–C31–P2/P1–C15–P2 planes in **16** and **18** are 84.31° and 82.76°. The metal centres in complexes **16–18** (Fig. 5 and 6) adopt slightly distorted square planar geometries. The P1–M1–P2 bite angles in **16** and **18** [93.69(3)°, 94.62(3)°] are smaller than those found in analogous eight-membered chelate complexes $[\text{PdCl}_2\text{dppf}]$ and $[\text{PdCl}_2\{\text{Ph}_2\text{PC}_6\text{H}_4\text{OC}_6\text{H}_4\text{PPh}_2\text{-}\kappa^2\text{P,P}\}]$ (99.07° and 100.82° respectively) but are quite close to those for $[\text{PdCl}_2\{\text{P}\text{r}\text{P}\text{-}\kappa^2\text{P,P}\}]$ (93.22°) [P_rP = 1,2-bis(2-diphenylphosphinoimidazol-1-yl)benzene].^{9c,25,26} The decrease in the bite angles of **16** and **17** compared to that of $[\text{PdCl}_2\{\text{Ph}_2\text{PC}_6\text{H}_4\text{OC}_6\text{H}_4\text{PPh}_2\text{-}\kappa^2\text{P,P}\}]$ may be due to the presence of a flexible CH₂ bridge as it allows the two PPh₂-appended heterocyclic rings to come closer to each other. The Cl1–M1–Cl2 bond angles in **16** and **17** [92.31(3)° and 90.31(3)°] are larger than those observed in $[\text{PdCl}_2(\text{dppb-}\kappa^2\text{P,P})]$ [88.21°] and $[\text{PdCl}_2(\text{dppf})]$ [87.8°], but are comparable to the values found in $[\text{PdCl}_2(\text{dppe-}\kappa^2\text{P,P})]$ [94.2°] and $[\text{PdCl}_2(\text{dppp-}\kappa^2\text{P,P})]$ [90.8°].²⁷ The average Pd–P bond distances in **16** and **17** [2.2515(4) Å and 2.26348(5) Å] are slightly shorter than those found in complexes $[\text{PdCl}_2(\text{Xantphos-}\kappa^2\text{P,P})]$



Scheme 4 Synthesis of palladium(II) complexes.

Table 3 Selected bond distances and bond angles for 16–18

	16	17	18
Bond distances (Å)			
M1–P1	2.2461(9)	2.2696(8)	2.2327(6)
M1–P2	2.2568(9)	2.2572(9)	2.2442(7)
M–Cl1	2.3597(9)	2.3495(8)	2.3420(6)
M–Cl2	2.3350(9)	2.3136(8)	2.3641(6)
Bond angles (°)			
P1–M1–P2	93.69(3)	94.62(3)	94.53(2)
Cl2–M1–Cl1	92.31(3)	90.31(3)	89.67(2)
Cl2–M1–P1	91.94(3)	172.97(3)	92.50(2)
Cl1–M1–P2	84.88(3)	168.30(3)	85.30(2)
Cl2–M1–P2	169.11(3)	92.37(3)	169.73(2)
Cl1–M1–P1	163.57(3)	82.70(3)	166.13(2)

(Pd–P_{avg} 2.295(3) Å) and [PdCl₂(dppf)] (Pd–P_{avg} 2.292(3) Å) indicating stronger metal to ligand bonding interaction.^{25,26,28}

The Pt–P bond distances [2.2327(6) Å, 2.2442(7) Å] and the P1–M1–P2 bond angle [94.53(2)°] in **18**, respectively, are shorter/smaller than those for [PtCl₂{(CH₂(1,2-C₃H₂N₂PPh₂))₂}-κ²P,P}] [2.252(2) Å, 2.269(5) Å; 98.85(10)°].^{8a}

In complex **21**, the bisphosphine **2** shows the bridging (μ-P, P) as well as chelating (κ²-P,N) modes of coordination (Fig. 7). The geometries around the Pd^{II} centres are distorted square

planar. The N4–Pd1–P1 [100.88(6)°] and N2–Pd2–P2 [98.50(6)°] bond angles are unequal in seven-membered chelate rings and are larger than the P1–Pd2–P2 bond angles found in eight-membered chelate complexes **16** and **17** with κ²-P,P coordination (Table 4). The Pd1–P1 [2.2927(7) Å and Pd2–P2 [2.3215(7) Å] bond distances are unequal and are shorter than those found in [Pd((CH₃)₂C₃H₃){Ph₂PC₆H₄OC₆H₄PPh₂-κ²P,P}][BF₄] [2.336(2) Å, 2.379(2) Å] and [Pd((CH₃)₂C₃H₃)(Xantphos-κ²P,P)][BF₄] [2.372(2) Å], but are comparable to those for [Pd((CH₃)₂C₃H₃)(dppf)][BF₄] [2.296(2) Å, 2.293(2) Å] and [Pd((CH₃)₂C₃H₃)(dppf)][BF₄] [2.313(6) Å, 2.33(9) Å].²⁹ The allyl moieties are coordinated in an asymmetric fashion to the Pd^{II} centres as reflected from the Pd–C bond lengths. The Pd–C bond lengths range from 2.124(8)–2.227(9) Å and the shortest Pd–C bonds are located as expected *trans* to the nitrogen donor atom.

Hydroformylation reactions

Hydroformylation of olefins to aldehydes is one of the most important transition metal catalysed C–C bond forming reactions. A significant number of catalyst systems based on various phosphorus based ligands have been examined as pre-catalysts for olefin hydroformylation³⁰ with rhodium complexes containing bisphosphines being ideal candidates for hydroformylation reactions. The utility of bis(azol-1-yl)

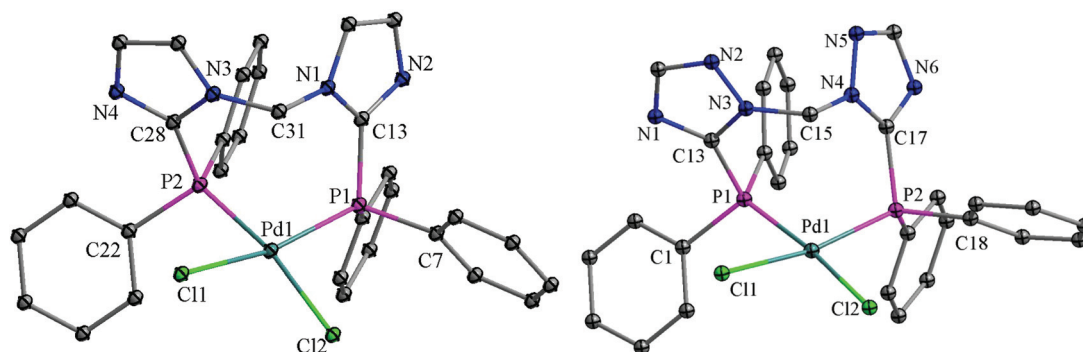


Fig. 5 Molecular structures of $[\text{PdCl}_2\{(\text{CH}_2(1,3\text{-C}_3\text{H}_2\text{N}_2\text{PPh}_2)_2)\text{-}\kappa^2\text{P,P}}]$ (**16**) and $[\text{PdCl}_2\{(\text{CH}_2(1,2,4\text{-C}_2\text{HN}_3\text{PPh}_2)_2)\text{-}\kappa^2\text{P,P}}]$ (**17**). Thermal ellipsoids are drawn at 50% probability level. Hydrogen atoms have been omitted for clarity.

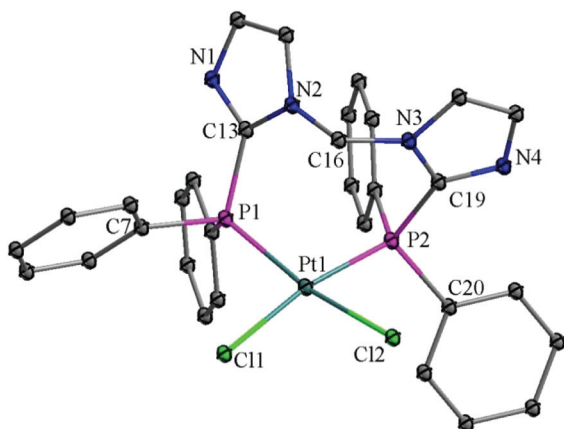


Fig. 6 Molecular structure of $[\text{PtCl}_2\{(\text{CH}_2(1,3\text{-C}_3\text{H}_2\text{N}_2\text{PPh}_2)_2)\text{-}\kappa^2\text{P,P}}]$ (**18**). Thermal ellipsoids are drawn at 50% probability level. Hydrogen atoms have been omitted for clarity.

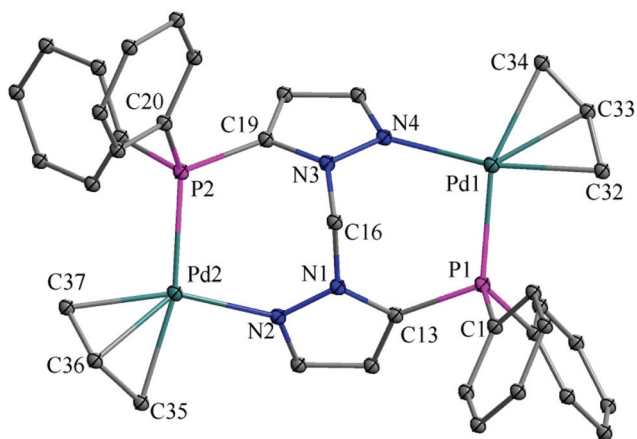


Fig. 7 Molecular structure of $[\text{Pd}_2(\eta^3\text{-C}_3\text{H}_5)_2\{(\text{CH}_2(1,2\text{-C}_3\text{H}_2\text{N}_2\text{PPh}_2)_2)\text{-}\kappa^2\text{P,N}}][\text{BF}_4]_2$ (**21**). Thermal ellipsoids are drawn at 50% probability level. Hydrogen atoms have been omitted for clarity.

methane-based bisphosphines in hydroformylation is not known. However, the catalytic activity of imidazolium substituted monophosphines with a π -acceptor character has been

Table 4 Selected bond distances and bond angles for **21**

Bond distances (Å)		Bond angles (°)	
Pd1–P1	2.2927(7)	N4–Pd1–P1	100.88(6)
Pd2–P2	2.3215(7)	N2–Pd1–P2	98.50(6)
Pd2–N2	2.086(2)	C32–Pd1–C34	66.0(4)
Pd1–N4	2.148(2)	C35–Pd2–C37	67.3(4)
Pd1–C32	2.124(8)	C32–Pd1–P1	93.9(3)
Pd1–C33	2.157(5)	C34–Pd1–N4	99.4(3)
Pd1–C34	2.227(9)	C35–Pd2–N2	95.3(3)
Pd2–C35	2.191(8)	C37–Pd2–P2	98.6(3)
Pd2–C36	2.170(4)		
Pd2–C37	2.133(8)		

investigated recently in the rhodium catalysed hydroformylation of alkenes.^{31–33}

The bisphosphines **1–3** were employed in the hydroformylation of olefins with the initial studies conducted using **1** with $[\text{Rh}(\text{acac})(\text{CO})_2]$ as a catalyst for hydroformylation of styrene as a model reaction. Since the isolated complexes **13–15** showed only moderate conversions with b : l ratio, so as the combination of ligands **2** and **3** with $[\text{Rh}(\text{acac})(\text{CO})_2]$, only the combination of ligand **1** and $[\text{Rh}(\text{acac})(\text{CO})_2]$ was considered for further investigation. The results are summarized in Table 8. The conversion of styrene increases with pressure (entries 2 and 3). It is also observed that the yield of product decreases with decrease in catalyst concentration (entries 3 and 4). From these, the standard reaction conditions for the catalytic runs were set at 60 °C and 40 bar of syn gas ($\text{H}_2/\text{CO} = 1 : 1$) for 7 h. The substrate to catalyst ratio and ligand to metal ratio were 1 : 1000 and 1 : 1. Noteworthy is the very good selectivity (84%) for the formation of the branched aldehyde (entry 3). Under identical reaction conditions, ligands **2** and **3** showed almost similar reaction rates but the regioselectivity decreased compared to **1** (entries 5 and 6). The optimized reaction conditions used in case of **1** were further applied for hydroformylation of various olefins with electron rich as well as electron deficient substituents which showed good conversion and selectivity to the desired product (Table 9). Under identical conditions PPh_3 showed 84% conversion with b : l ratio of 68 : 32. Bisphosphine **1** shows good catalytic efficiency.

Table 5 Crystallographic information for compounds 1, 2, 4 and 5

	1	2	4	5
Empirical formula	C ₃₁ H ₂₆ N ₄ P ₂	C ₃₁ H ₂₆ N ₄ P ₂ ·CHCl ₃	C ₃₁ H ₂₆ N ₄ P ₂ Se ₂	C ₃₁ H ₂₆ N ₄ P ₂ Se ₂
Fw	516.50	635.87	674.42	674.42
Cryst. system	Orthorhombic	Triclinic	Monoclinic	Monoclinic
Space group	P2 ₁ 2 ₁ 2 ₁ (no. 19)	P $\bar{1}$ (no.2)	P2 ₁ /n(no. 14)	P2 ₁ /c(no. 14)
a, Å	8.9713(7)	12.323(2)	13.075(3)	17.6873(6)
b, Å	10.3845(8)	12.892(2)	13.423(3)	9.4183(3)
c, Å	27.663(2)	12.951(2)	16.698(4)	18.1538(6)
α , °	90	93.935(2)	90	90
β , °	117.081(2)	117.423(2)	103.217(4)	109.520(1)
γ , °	90	117.267(2)	90	90
V, Å ³	2577.2(3)	1517.9(4)	2853.0(11)	2850.29(16)
Z	4	2	4	4
D _{calc} , g cm ⁻³	1.331	1.391	1.570	1.572
μ (Mo K α), mm ⁻¹	0.139	0.437	2.733	4.527
F(000)	1080	656	1352	1352
Crystal size, mm	0.12 × 0.12 × 0.19	0.16 × 0.18 × 0.20	0.15 × 0.18 × 0.24	0.04 × 0.16 × 0.2
T (K)	100	100	100	100
2 θ range, °	2.1–28.2	1.9–28.4	2.1–29.1	2.65–72.4
Total no. of reflns	83 301	26 708	49 639	48 861
No. of indep reflns	6350	7461	7417	43 796
S	1.05	1.04	1.03	1.038
R ₁	0.0332	0.0323	0.0284	0.0352
wR ₂	0.0847	0.0858	0.0730	0.0728

Table 6 Crystallographic information for compounds 6 and 10–12

	6	10	11	12
Empirical formula	C ₂₉ H ₂₄ N ₆ P ₂ Se ₂	C ₃₆ H ₃₁ ClN ₄ P ₂ Ru	C ₃₆ H ₃₁ ClN ₄ P ₂ Ru	C ₃₅ H ₃₁ Cl ₃ N ₆ P ₂ Ru
Fw	676.40	718.11	718.11	805.02
Cryst. system	Monoclinic	Monoclinic	Triclinic	Triclinic
Space group	P2 ₁ /n(no. 14)	P2 ₁ /n(no. 14)	P $\bar{1}$	P $\bar{1}$
a, Å	14.321(3)	11.0252(13)	9.1612(3)	9.4977(3)
b, Å	11.432(2)	25.073(3)	12.9584(5)	18.3954(4)
c, Å	17.924(3)	11.0932(13)	15.8185(3)	19.9460(5)
α , °	90	90	98.610(2)	87.8663(17)
β , °	103.979(2)	90.325(2)	92.840(2)	79.437(2)
γ , °	90	90	107.317(3)	78.663(2)
V, Å ³	2847.6(9)	3066.5(6)	1763.73(10)	3358.93(15)
Z	4	4	2	4
D _{calc} , g cm ⁻³	1.578	1.556	1.352	1.592
μ (Mo K α), mm ⁻¹	2.740	0.737	0.641	0.838
F(000)	1352	1464	732	1632
Crystal size, mm	0.10 × 0.11 × 0.24	0.08 × 0.14 × 0.14	0.27 × 0.22 × 0.14	0.29 × 0.14 × 0.08
T (K)	150	100	150(2)	150(2)
2 θ range, °	2.3–27.01	2.0–29.1	2.72–25.00	2.22–25.00
Total no. of reflns	42 623	54 370	14 246	57 268
No. of indep reflns	22 031	8058	6160	11 835
S	1.041	1.05	1.055	1.039
R ₁	0.1641	0.0293	0.0380	0.0298
wR ₂	0.2389	0.0773	0.1014	0.0651

Conclusions

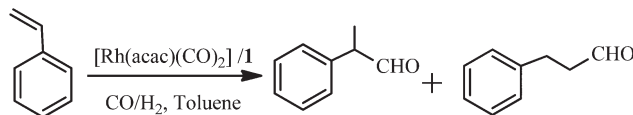
The coordination behaviour of bisphosphines 1–3 towards Ru^{II}, Rh^I, Pd^{II} and Pt^{II} has been described. Ligand 1 forms chelate (κ^2 -P,P) complexes with Ru^{II}, Rh^I, Pd^{II} and Pt^{II}, whereas ligands 2 and 3 show both κ^2 -P,P or κ^2 -P,N modes of coordination. The formation of dinuclear complexes through κ^2 -P,N coordination in 2 and 3 is due to the free rotation of phosphine-appended heterocyclic rings around the central methylene carbon. Unlike typical large bite ligands which always

show larger bite angles at the metal centers irrespective of the nature of the metal and its geometry, the ligands in the present investigation have displayed their ability to vary the bite angles from 88 to 115° which is a promising feature in homogeneous catalysis where bite angles play a prominent role. The *in situ* generated Rh^I complex of 1 catalyses the hydroformylation of styrene with moderate selectivity. Due to the rotational fluxionality of the phosphine moieties and the ability of the ligands to show a κ^2 -P,N coordination mode, it is still possible to activate the C–H bond(s) of bridging methyl-

Table 7 Crystallographic information for compounds 14, 16–18 and 21

	14	16	17	18	21
Empirical formula	C ₄₇ H ₅₀ B ₂ F ₈ N ₄ P ₂ Rh ₂	C ₃₁ H ₂₆ C ₁₂ N ₄ P ₂ Pd	C ₂₉ H ₂₄ Cl ₂ N ₆ P ₂ Pd	C ₃₁ H ₂₆ Cl ₂ N ₄ P ₂ Pt	C ₃₇ H ₃₆ B ₂ F ₈ N ₄ P ₂ Pd ₂ ·CH ₂ Cl ₂
Fw	1112.29	693.80	695.78	782.49	1069.98
Cryst. System	Monoclinic	Monoclinic	Monoclinic	Monoclinic	Monoclinic
Space group	C2 (no. 5)	P2 ₁ /n (no. 14)	P2 ₁ /n (no. 14)	P2 ₁ /c (no. 14)	P2 ₁ /n (no. 14)
a, Å	15.8580(3)	12.041(4)	9.9501(3)	12.0662(8)	11.1418(5)
b, Å	11.7581(3)	18.039(6)	24.6633(9)	18.1114(12)	31.8019(15)
c, Å	13.3446(3)	13.169(4)	11.4922(4)	13.1999(9)	11.9253(6)
α, °	90	90	90	90	90
β, °	108.8490(6)	92.438(40)	98.4310(16)	92.314(1)	102.2500(7)
γ, °	90	90	90	90	90
V, Å ³	2354.80(9)	2857.8(16)	2789.73(16)	2882.3(3)	4129.3(3)
Z	2	4	4	4	4
D _{calc} , g cm ⁻³	1.569	1.613	1.657	1.803	1.721
μ (Mo Kα), mm ⁻¹	6.912	0.978	8.474	5.194	1.15
F(000)	1124	1400	1400	1528	2128
Crystal size, mm	0.030 × 0.090 × 0.13	0.03 × 0.13 × 0.16	0.03 × 0.05 × 0.2	0.14 × 0.19 × 0.23	0.07 × 0.14 × 0.16
T (K)	100(2)	100	100	100	150(2)
2θ range, °	3.5–72.18	1.7–28.5	3.5–72.5	1.9–29.2	2.362–29.118
Total no. of reflns	4256	24 568	10 351	50 599	10 965
No. of indep reflns	4209	6702	4324	7536	9158
S	1.062	1.03	0.988	1.03	1.042
R ₁	0.0226	0.0355	0.0512	0.0221	0.0477
wR ₂	0.0568	0.0959	0.0675	0.0523	0.0825

Table 8 Hydroformylation of styrene using bisphosphines 1–3



Entry	Compound	P (Bar)	Time (h)	Conversion (%)	Branched : linear	TON
1	1	30	6	91	75 : 25	910
2	1	30	7	90	82 : 18	900
3 ^a	1	40	7	99	84 : 16	990
4 ^b	1	40	7	96	69 : 31	480
5 ^a	2	40	7	98	72 : 28	980
6 ^a	3	40	7	96	78 : 22	960
7	PPh ₃	40	9	84	68 : 32	840
8	13	20	9	70	65 : 35	700
9	14	20	9	88	61 : 39	880
10	15	20	9	92	62 : 38	920

Temp. = 60 °C, solvent = toluene. ^a S/C = 1000. ^b S/C = 2000.

ene groups to form interesting pincer complexes. Further work in this direction and also further exploration of these ligands in other catalytic reactions are in progress.

Experimental section

General procedures

All experimental manipulations were performed under an inert atmosphere of dry nitrogen or argon, using standard Schlenk techniques. All the solvents were purified by conventional procedures and distilled prior to use. The compounds bis(azol-1-yl)methane (imidazole, pyrazole, 1,2,4-triazole),³⁴ ligands 1–3,^{8a–c} [Ru(η⁶-cymene)Cl₂]₂,³⁵ [(η⁵-C₅H₅)RuCl(PPh₃)₂],³⁶ [Rh(COD)Cl]₂,³⁷ [M(COD)Cl₂] (M = Pd or Pt),³⁸ and [Pd(η³-C₃H₅)Cl]₂,³⁹ were

Table 9 Hydroformylation of styrene and its derivatives

Entry	Substrate	Conversion	Branched : linear	TON
1	Styrene	99	84 : 16	990
2	4- <i>tert</i> -Butyl styrene	99	73 : 27	990
3	3-Methyl styrene	99	72 : 28	990
4	4-Cl styrene	99	83 : 17	990
5	4-Br styrene	98	76 : 24	980

Temp. = 60 °C, pressure = 40 bar (1 : 1/CO : H₂), time = 7 h, solvent = toluene, S/C = 1000.

prepared according to the published procedures. Other reagents were obtained from commercial sources and used after purification.

Instrumentation

Solution NMR spectra were recorded on a Bruker AV-400 or AV-500 MHz spectrometer at ambient probe temperatures. NMR shifts are given in δ with positive values downfield of tetramethylsilane (^1H) and external 85% H_3PO_4 (^{31}P). The ^{31}P NMR spectra were recorded in a proton-decoupled mode. Positive values indicate downfield shifts. Microanalyses were carried out using a Carlo Erba (model 1106) elemental analyzer. Melting points of all compounds were determined on a Veego melting point apparatus and are uncorrected.

Synthesis of $[\text{CH}_2(1,3\text{-C}_3\text{H}_2\text{N}_2\text{PPh}_2\text{Se})_2]$ (4)

A mixture of **1** (30 mg, 0.058 mmol) and elemental selenium (9.1 mg, 0.116 mmol) in toluene (15 mL) was refluxed for 12 h. The colourless solution was filtered through a frit containing Celite. The filtrate was reduced to 5 mL and layered with petroleum ether to give colourless X-ray quality crystals of **4**. Yield: 64% (25 mg). Mp: 185 °C. ^1H NMR (400 MHz, CDCl_3): δ 6.98 (s, 2H, CH_2), 7.17 (s, 2H, H^4), 7.44–7.51 (m, 22H, H^5 , ArH). $^{31}\text{P}\{^1\text{H}\}$ NMR (162 MHz, CDCl_3): δ 17.8 (s, $^1J_{\text{PSe}} = 729$ Hz). Anal. Calcd for $\text{C}_{31}\text{H}_{26}\text{N}_4\text{P}_2\text{Se}_2$: C, 55.21; H, 3.89; N, 8.31. Found: C, 55.17; H, 3.78; N, 8.38%.

Synthesis of $[\text{CH}_2(1,2\text{-C}_3\text{H}_2\text{N}_2\text{PPh}_2\text{Se})_2]$ (5)

This was synthesized by a procedure similar to that of **4** using **2** (40 mg, 0.077 mmol) and elemental selenium (12 mg, 0.15 mmol). Yield: 76% (52 mg). Mp: 265–268 °C. ^1H NMR (400 MHz, CDCl_3): δ 5.89 (s, 2H, $^2J_{\text{HH}} = 2$ Hz, H^3), 7.04 (s, 2H, CH_2), 7.30 (t, 2H, H^4), 7.42–7.77 (m, 20H, ArH). $^{31}\text{P}\{^1\text{H}\}$ NMR (162 MHz, CDCl_3): δ 15.7 (s, $^1J_{\text{PSe}} = 746.7$ Hz). Anal. Calcd for $\text{C}_{31}\text{H}_{26}\text{N}_4\text{P}_2\text{Se}_2$: C, 55.21; H, 3.89; N, 8.31. Found: C, 55.32; H, 3.71; N, 8.40%.

Synthesis of $[\text{CH}_2(1,2,4\text{-C}_2\text{HN}_3\text{PPh}_2\text{Se})_2]$ (6)

This was synthesized by a procedure similar to that of **4** using **3** (40 mg, 0.079 mmol) and elemental selenium (12 mg, 0.16 mmol). Yield: 74% (42 mg). Mp: 234 °C. ^1H NMR (400 MHz, CDCl_3): δ 7.71 (s, 2H, CH_2), 7.73 (s, 2H, H^3), 7.45–7.84 (m, 20H, ArH). $^{31}\text{P}\{^1\text{H}\}$ NMR (162 MHz, CDCl_3): δ 17.9 (s, $^1J_{\text{PSe}} = 754$ Hz). Anal. Calcd for $\text{C}_{29}\text{H}_{24}\text{N}_6\text{P}_2\text{Se}_2$: C, 51.49; H, 3.58; N, 12.42. Found: C, 51.57; H, 3.47; N, 12.51%.

Synthesis of $[\text{Ru}_2\text{Cl}_4(\eta^6\text{-}p\text{-cymene})_2\{\mu\text{-}(\text{CH}_2(1,3\text{-C}_3\text{H}_2\text{N}_2\text{PPh}_2)_2)\text{-}\kappa^2\text{P,P}\}]$ (7)

A solution of $[\text{Ru}(\eta^6\text{-}p\text{-cymene})\text{Cl}_2]_2$ (35 mg, 0.058 mmol) in CH_2Cl_2 (10 mL) was added dropwise to a solution of **1** (30 mg, 0.058 mmol) in CH_2Cl_2 (10 mL) at room temperature. The red solution obtained was stirred for 5 h. The solvent was evaporated under reduced pressure and the residue was washed with diethyl ether to afford the analytically pure product of **7** as a brick red solid. Yield: 78.5% (51 mg). Mp: >280 °C. ^1H NMR (400 MHz, CDCl_3): δ 6.87 (s, 2H, CH_2), 7.15 (s, 2H, H^4), 7.26–7.89 (m, 22H, H^3 , ArH), 0.98 (d, 6H, $^3J_{\text{HH}} = 6.9$ Hz, $^1\text{Pr-CH}_3$), 1.01 (d, 6H, $^3J_{\text{HH}} = 6.9$ Hz, $^1\text{Pr-CH}_3$), 1.67 (s, 6H, $p\text{-CH}_3$), 2.60 (sep, 2H, $^1\text{Pr-CH}$), 5.31 (d, 2H, $^3J_{\text{HH}} = 6.1$ Hz, Ph-CH), 5.18

(d, 2H, $^3J_{\text{HH}} = 6.1$ Hz, Ph-CH), 5.13 (d, 2H, $^3J_{\text{HH}} = 6.1$ Hz, Ph-CH), 5.09 (s, 2H, Ph-CH). $^{31}\text{P}\{^1\text{H}\}$ NMR (162 MHz, CDCl_3): δ 11.3 (s). Anal. Calcd for $\text{C}_{51}\text{H}_{54}\text{N}_4\text{P}_2\text{Ru}_2$: C, 62.02; H, 5.51; N, 5.68. Found: C, 62.12; H, 5.45; N, 5.61%.

Synthesis of $[\text{Ru}_2\text{Cl}_4(\eta^6\text{-}p\text{-cymene})_2\{\mu\text{-}(\text{CH}_2(1,2\text{-C}_3\text{H}_2\text{N}_2\text{PPh}_2)_2)\text{-}\kappa^2\text{P,P}\}]$ (8)

This was synthesized by a procedure similar to that of **7** using **2** (20 mg, 0.038 mmol) and $[\text{Ru}(\eta^6\text{-}p\text{-cymene})\text{Cl}_2]_2$ (24 mg, 0.038 mmol). Yield: 79.5% (35 mg). Mp: >280 °C. ^1H NMR (400 MHz, CDCl_3): δ 6.45 (m, 2H, CH_2), 6.31 (m, 2H, H^4), 7.70 (m, 2H, H^3), 7.05–7.95 (m, 20H, ArH), 1.41 (d, 6H, $^3J_{\text{HH}} = 6.9$ Hz, $^1\text{Pr-CH}_3$), 1.32 (d, 6H, $^3J_{\text{HH}} = 6.9$ Hz, $^1\text{Pr-CH}_3$), 1.89 (s, 6H, $p\text{-CH}_3$), 3.18 (sep, 2H, $^1\text{Pr-CH}$), 5.811 (d, 4H, $^3J_{\text{HH}} = 6.1$ Hz, Ph-CH), 4.7 (4H, Ph-CH). $^{31}\text{P}\{^1\text{H}\}$ NMR (162 MHz, CDCl_3): δ 15.8 (s). Anal. Calcd for $\text{C}_{51}\text{H}_{54}\text{N}_4\text{P}_2\text{Ru}_2\text{-CH}_2\text{Cl}_2$: C, 58.26; H, 5.27; N, 5.23. Found: C, 58.35; H, 5.18; N, 5.12%.

Synthesis of $[\text{Ru}_2\text{Cl}_4(\eta^6\text{-}p\text{-cymene})_2\{\mu\text{-}(\text{CH}_2(1,2,4\text{-C}_2\text{HN}_3\text{PPh}_2)_2)\text{-}\kappa^2\text{P,P}\}]$ (9)

This was synthesized by a procedure similar to that of **7** using **3** (25 mg, 0.048 mmol) and $[\text{Ru}(\eta^6\text{-}p\text{-cymene})\text{Cl}_2]_2$ (29 mg, 0.048 mmol). Yield: 72.5% (39 mg). Mp: >280 °C. ^1H NMR (400 MHz, CDCl_3): δ 6.09 (s, 2H, CH_2), 8.12 (s, 2H, H^4), 7.16–8.10 (m, 20H, ArH), 1.17 (d, 6H, $^3J_{\text{HH}} = 6.9$ Hz, $^1\text{Pr-CH}_3$), 1.20 (d, 6H, $^3J_{\text{HH}} = 6.9$ Hz, $^1\text{Pr-CH}_3$), 1.82 (s, 6H, $p\text{-CH}_3$), 2.85 (sep, 2H, $^1\text{Pr-CH}$), 5.59 (d, 2H, $^2J_{\text{HH}} = 6.1$ Hz, Ph-CH), 5.54 (d, 2H, $^3J_{\text{HH}} = 6.2$ Hz, Ph-CH), 5.28 (d, 2H, $^3J_{\text{HH}} = 6.1$ Hz, Ph-CH), 4.89 (d, 2H, $^3J_{\text{HH}} = 6.1$ Hz, Ph-CH). $^{31}\text{P}\{^1\text{H}\}$ NMR (162 MHz, CDCl_3): δ 13.7 (s). Anal. Calcd for $\text{C}_{49}\text{H}_{52}\text{Cl}_4\text{N}_6\text{P}_2\text{Ru}_2$: C, 52.04; H, 4.63; N, 7.43. Found: C, 52.15; H, 4.52; N, 7.57%.

Synthesis of $[(\eta^5\text{-C}_5\text{H}_5)\text{RuCl}\{(\text{CH}_2(1,3\text{-C}_3\text{H}_2\text{N}_2\text{PPh}_2)_2)\text{-}\kappa^2\text{P,P}\}]$ (10)

A solution of $[(\eta^5\text{-C}_5\text{H}_5)\text{RuCl}(\text{PPh}_3)_2]$ (35 mg, 0.048 mmol) in toluene (10 mL) was added slowly to a solution of **1** (25 mg, 0.048 mmol) in toluene (10 mL) at room temperature and the mixture was heated at 100 °C for 12 h to give a clear yellow solution. The solvent was evaporated under reduced pressure and the residue obtained was washed with petroleum ether several times. The residue was dissolved in CH_2Cl_2 and layered with petroleum ether, which on slow evaporation gave red crystals of **10**. Yield: 76.5% (26 mg). Mp: 251–254 °C. ^1H NMR (400 MHz, CDCl_3): δ 5.24 (d, 1H, $^2J_{\text{HH}} = 14.4$ Hz, CH_2), 7.13 (s, 1H, $^2J_{\text{HH}} = 14.4$ Hz, CH_2), 6.93 (s, 2H, H^5), 6.98 (s, 2H, H^4), 7.26–7.53 (m, 20H, ArH), 4.17 (s, 5H, C_5H_5). $^{31}\text{P}\{^1\text{H}\}$ NMR (162 MHz, CDCl_3): δ 41.2 (s). Anal. Calcd for $\text{C}_{36}\text{H}_{31}\text{ClN}_4\text{P}_2\text{Ru}$: C, 60.21; H, 4.35; N, 7.80. Found: C, 60.28; H, 4.26; N, 7.76%.

Synthesis of $[(\eta^5\text{-C}_5\text{H}_5)\text{RuCl}\{(\text{CH}_2(1,2\text{-C}_3\text{H}_2\text{N}_2\text{PPh}_2)_2)\text{-}\kappa^2\text{P,P}\}]$ (11)

This was synthesized by a procedure similar to that of **10** using **2** (20 mg, 0.038 mmol) and $[(\eta^5\text{-C}_5\text{H}_5)\text{RuCl}(\text{PPh}_3)_2]$ (28 mg, 0.038 mmol). Yield: 75.2% (21 mg). Mp: 275 °C. ^1H NMR (400 MHz, CDCl_3): δ 5.99 (d, 1H, $^2J_{\text{HH}} = 14.4$ Hz, CH_2), 7.07 (s, 1H, $^2J_{\text{HH}} = 14.4$ Hz, CH_2), 5.54 (br, 2H, H^4), 6.71 (s, 2H, H^3), 7.21–7.58 (m, 20H, ArH), 4.28 (s, 5H, C_5H_5). $^{31}\text{P}\{^1\text{H}\}$ NMR

(162 MHz, CDCl₃): δ 36.4 (s). Anal. Calcd for C₃₆H₃₁ClN₄P₂Ru: C, 60.21; H, 4.35; N, 7.80. Found: C, 60.27; H, 4.21; N, 7.65%.

Synthesis of $[(\eta^5\text{-C}_5\text{H}_5)\text{RuCl}(\text{CH}_2(1,2,4\text{-C}_2\text{HN}_3\text{PPh}_2)_2)\text{-}\kappa^2\text{P,P}']$ (12)

This was synthesized by a procedure similar to that of **10** using **3** (20 mg, 0.038 mmol) and $[(\eta^5\text{-C}_5\text{H}_5)\text{RuCl}(\text{PPh}_3)_2]$ (28 mg, 0.038 mmol). Yield: 75% (21 mg). Mp: 272–276 °C. ¹H NMR (400 MHz, CDCl₃): δ 5.99 (d, 1H, ²J_{HH} = 14.4 Hz, CH₂), 7.18 (s, 1H, ²J_{HH} = 14.4 Hz, CH₂), 6.91–7.51 (m, 20H, ArH), 7.74 (s, 2H, H³), 4.27 (s, 5H, C₅H₅). ³¹P{¹H} NMR (162 MHz, CDCl₃): δ 42.3 (s). Anal. Calcd for C₃₄H₂₉ClN₆P₂Ru: C, 56.71; H, 4.06; N, 11.67. Found: C, 56.52; H, 3.95; N, 11.52%.

Synthesis of $[\text{Rh}(\text{COD})\{(\text{CH}_2(1,3\text{-C}_3\text{H}_2\text{N}_2\text{PPh}_2)_2)\text{-}\kappa^2\text{P,P}']\text{BF}_4$ (13)

To a stirred solution of $[\text{Rh}(\text{COD})\text{Cl}]_2$ (10 mg, 0.02 mmol) in THF (10 mL), AgBF₄ (8 mg, 0.04 mmol) was added. After 30 minutes, the suspension obtained was filtered to remove AgCl, and a solution of ligand **1** (20 mg, 0.04 mmol) in THF (6 mL) was added drop-wise and the mixture was stirred for 2 h. The yellow coloured solution was evaporated under reduced pressure and the residue was washed with petroleum ether to afford the analytically pure product of **13** as a yellow solid. Yield: 64% (31 mg). Mp: 194–198 °C. ¹H NMR (400 MHz, CDCl₃): δ 7.85 (s, 2H, H⁵), 7.22–7.56 (m, 24H, CH², H⁴, ArH), 4.71 (br s, 4H, COD), 2.52 (br s, 4H, COD), 2.34 (br s, 4H, COD). ³¹P{¹H} NMR (162 MHz, CDCl₃): δ 3.2 (s, ¹J_{PRh} = 140.8 Hz). Anal. Calcd for C₃₉H₃₈N₄P₂RhBF₄: C, 57.52; H, 4.70; N, 6.88. Found: C, 57.42; H, 4.64; N, 6.75%.

Synthesis of $[\text{Rh}_2(\text{COD})_2\{(\text{CH}_2(1,2\text{-C}_3\text{H}_2\text{N}_2\text{PPh}_2)_2)\text{-}\kappa^2\text{P,N}'](\text{BF}_4)_2$ (14)

This was synthesized by a procedure similar to that of **13** using **2** (20 mg, 0.04 mmol) and $[\text{Rh}(\text{COD})\text{Cl}]_2$ (20 mg, 0.04 mmol) and AgBF₄ (16 mg, 0.08 mmol). Yield: 65% (28 mg). Mp: 183–187 °C. ¹H NMR (400 MHz, DMSO-*d*₆): δ 7.22 (s, 2H, CH₂), 6.77 (s, 2H, H⁴), 8.91 (s, 2H, H³), 7.26–8.22 (m, 20H, ArH), 5.65 (br s, 8H, COD), 2.14 (br s, 8H, COD), 2.01 (br s, 8H, COD). ³¹P{¹H} NMR (162 MHz, DMSO-*d*₆): δ 3.8 (d, ¹J_{PRh} = 148.9 Hz). Anal. Calcd for C₄₇H₅₀N₄P₂Rh₂B₂F₈: C, 50.75; H, 4.53; N, 5.05. Found: C, 50.68; H, 4.42; N, 4.83%.

Synthesis of $[\text{Rh}_2(\text{COD})_2\{(\text{CH}_2(1,2,4\text{-C}_2\text{HN}_3\text{PPh}_2)_2)\text{-}\kappa^2\text{P,N}'](\text{BF}_4)_2$ (15)

This was synthesized by a procedure similar to that of **13** using **3** (20 mg, 0.038 mmol) and $[\text{Rh}(\text{COD})\text{Cl}]_2$ (20 mg, 0.038 mmol) and AgBF₄ (15 mg, 0.077 mmol). Yield: 61% (25 mg). Mp: 210 °C. ¹H NMR (400 MHz, DMSO-*d*₆): δ : 8.89 (s, 2H, H³), 7.19–7.99 (m, 22H, CH₂, ArH), 4.46 (br s, 8H, COD), 2.41 (br s, 8H, COD), 2.12 (br s, 8H, COD). ³¹P{¹H} NMR (162 MHz, DMSO-*d*₆): δ 29.1 (s, ¹J_{PRh} = 168.4 Hz). Anal. Calcd for C₄₅H₄₈N₆P₂Rh₂B₂F₈: C, 48.51; H, 4.34; N, 7.54. Found: C, 48.43; H, 4.27; N, 7.46%.

Synthesis of $[\text{PdCl}_2\{(\text{CH}_2(1,3\text{-C}_3\text{H}_2\text{N}_2\text{PPh}_2)_2)\text{-}\kappa^2\text{P,P}']$ (16)

A solution of Pd(COD)Cl₂ (12 mg, 0.058 mmol) in CH₂Cl₂ (10 mL) was added dropwise to a solution of **1** (30 mg, 0.058 mmol) also in CH₂Cl₂ (10 mL). The resultant clear yellow solution was reduced to 5 mL and layered with diethyl ether to

generate yellow coloured X-ray quality crystals of **16**. Yield: 71% (32 mg). Mp: 254–256 °C. ¹H NMR (400 MHz, DMSO-*d*₆): δ 5.73 (s, 2H, CH₂), 8.10 (s, 2H, H⁵), 7.19–7.37 (m, 22H, H⁴, ArH). ³¹P{¹H} NMR (162 MHz, DMSO-*d*₆): δ 11.8 (s). Anal. Calcd for C₃₁H₂₆N₄P₂PdCl₂: C, 53.66; H, 3.78; N, 8.07. Found: C, 53.55; H, 3.81; N, 7.82%.

Synthesis of $[\text{PdCl}_2\{(\text{CH}_2(1,2,4\text{-C}_2\text{HN}_3\text{PPh}_2)_2)\text{-}\kappa^2\text{P,P}']$ (17)

This was synthesized by a procedure similar to that of **16** using **3** (30 mg, 0.058 mmol) and Pd(COD)Cl₂ (16 mg, 0.058 mmol). Yield: 82% (33 mg). Mp: >280 °C. ¹H NMR (400 MHz, DMSO-*d*₆): δ 5.73 (s, 2H, CH₂), 8.45 (s, 2H, H⁴), 7.26–7.47 (m, 20H, ArH). ³¹P{¹H} NMR (162 MHz, DMSO-*d*₆): δ 8.0 (s). Anal. Calcd for C₂₉H₂₄N₆P₂PdCl₂: C, 50.06; H, 3.48; N, 12.08. Found: C, 49.95; H, 3.52; N, 11.86%.

Synthesis of $[\text{PtCl}_2\{(\text{CH}_2(1,3\text{-C}_3\text{H}_2\text{N}_2\text{PPh}_2)_2)\text{-}\kappa^2\text{P,P}']$ (18)

A solution of Pt(COD)Cl₂ (21 mg, 0.058 mmol) in CH₂Cl₂ (10 mL) was added dropwise to a solution of **1** (30 mg, 0.058 mmol) also in CH₂Cl₂ (10 mL). The resultant colourless solution was reduced to 5 mL and layered with diethyl ether to form colourless X-ray quality crystals of **18**. Yield: 66.6% (30 mg). Mp: >280 °C. ¹H NMR (400 MHz, DMSO-*d*₆): δ 5.75 (s, 2H, CH₂), 8.11 (s, 2H, H⁵), 7.19–7.37 (m, 22H, H⁴, ArH). ³¹P{¹H} NMR (162 MHz, DMSO-*d*₆): δ -9.9 (s, ¹J_{PTp} = 3454 Hz). Anal. Calcd for C₃₁H₂₆N₄P₂PtCl₂: C, 47.58; H, 3.35; N, 7.16. Found: C, 47.44; H, 3.30; N, 7.17%.

Synthesis of $[\text{PtCl}_2\{(\text{CH}_2(1,2,4\text{-C}_2\text{HN}_3\text{PPh}_2)_2)\text{-}\kappa^2\text{P,P}']$ (19)

This was synthesized by a procedure similar to that of **17** using **3** (30 mg, 0.058 mmol) and Pt(COD)Cl₂ (21 mg, 0.058 mmol). Yield: 80% (35 mg). Mp: >280 °C. ¹H NMR (400 MHz, DMSO-*d*₆): δ 5.73 (s, 2H, CH₂), 8.43 (s, 2H, H⁴), 7.26–7.47 (m, 20H, ArH). ³¹P{¹H} NMR (162 MHz, DMSO-*d*₆): δ -7.4 (s, ¹J_{PTp} = 3473 Hz). Anal. Calcd for C₂₉H₂₄N₆P₂PtCl₂.CH₂Cl₂: 41.44; H, 3.01; N, 9.66. Found: C, 41.49; H, 2.85; N, 9.53%.

Synthesis of $[\text{Pd}(\eta^3\text{-C}_3\text{H}_5)\{(\text{CH}_2(1,3\text{-C}_3\text{H}_2\text{N}_2\text{PPh}_2)_2)\text{-}\kappa^2\text{P,P}']\text{OTf}$ (20)

A solution of $[(\eta^3\text{-C}_3\text{H}_5)\text{PdCl}]_2$ (10 mg, 0.03 mmol) in THF (10 mL) was added dropwise to a well stirred solution of AgOTf (15 mg, 0.06 mmol) in THF (5 mL). After 15 minutes, the suspension was filtered to remove AgCl and ligand **1** (30 mg, 0.06 mmol) in THF (8 mL) was added dropwise and the mixture was stirred for an additional 2 h. The solution was evaporated under reduced pressure and the residue washed with petroleum ether to afford the analytically pure product of **20** as a pale orange solid. Yield: 64% (30 mg), Mp: 204–208 °C. ¹H NMR (400 MHz, CDCl₃): δ 5.91 (s, 2H, CH₂), 7.12–7.42 (m, 24H, H⁴, H⁵, ArH), 3.48 (s, 1H, allyl), 4.15 (s, 2H, allyl), 5.31 (s, 2H, allyl). ³¹P{¹H} NMR (162 MHz, CDCl₃): δ 0.01 (s). Anal. Calcd for C₃₅H₃₁F₃N₄O₃P₂PdS: C, 51.70; H, 3.84; N, 6.89; S, 3.94. Found: C, 51.58; H, 3.79; N, 6.84; S, 3.87%.

Synthesis of $[\text{Pd}_2(\eta^3\text{-C}_3\text{H}_5)_2\{(\text{CH}_2(1,2\text{-C}_3\text{H}_2\text{N}_2\text{PPh}_2)_2)\text{-}\kappa^2\text{P,N}\}] (\text{BF}_4)_2$ (**21**)

This was synthesized by a procedure similar to that of **20** using **2** (30 mg, 0.06 mmol), $[(\eta^3\text{-C}_3\text{H}_5)\text{PdCl}]_2$ (22 mg, 0.06 mmol) and AgBF_4 (23 mg, 0.12 mmol). Yield: 53% (29 mg), Mp: 220 °C. ^1H NMR (400 MHz, CDCl_3): δ 6.84–8.12 (m, 26H, CH_2 , H^4 , H^3 , ArH), 4.04 (s, 2H, allyl), 4.45 (s, 4H, allyl), 6.09 (s, 4H, allyl). $^{31}\text{P}\{^1\text{H}\}$ NMR (162 MHz, CDCl_3): δ 8.7 (s). Anal. Calcd for $\text{C}_{37}\text{H}_{36}\text{N}_4\text{P}_2\text{Pd}_2\text{B}_2\text{F}_8\cdot\text{CH}_2\text{Cl}_2$: C, 42.65; H, 3.58; N, 5.24. Found: C, 42.44; H, 3.55; N, 5.11%.

Synthesis of $[\text{Pd}_2(\eta^3\text{-C}_3\text{H}_5)_2\{(\text{CH}_2(1,2,4\text{-C}_2\text{HN}_3\text{PPh}_2)_2)\text{-}\kappa^2\text{P,N}\}] (\text{BF}_4)_2$ (**22**)

This was synthesized by a procedure similar to that of **20** using **3** (30 mg, 0.06 mmol), $[(\eta^3\text{-C}_3\text{H}_5)\text{PdCl}]_2$ (22 mg, 0.06 mmol) and AgBF_4 (23 mg, 0.12 mmol). Yield: 54% (31 mg), Mp: 235–238 °C. ^1H NMR (400 MHz, CDCl_3): δ 7.26–8.51 (m, 26H, CH_2 , H^3 , ArH), 4.15 (s, 2H, allyl), 4.43 (s, 4H, allyl), 6.09 (br s, 4H, allyl). $^{31}\text{P}\{^1\text{H}\}$ NMR (162 MHz, CDCl_3): δ 11.3 (s). Anal. Calcd for $\text{C}_{35}\text{H}_{34}\text{N}_6\text{P}_2\text{Pd}_2\text{B}_2\text{F}_8$: C, 42.59; H, 3.47; N, 8.51. Found: C, 42.42; H, 3.23; N, 8.42%.

General procedure for hydroformylation reactions

In a typical hydroformylation reaction, a high pressure reactor of 100 mL capacity was charged with the ligand (5 μmol , 2.6 mg), $[\text{Rh}(\text{acac})(\text{CO})_2]$ (5 μmol , 1.4 mg) and olefin (5 mmol) in 20 mL of toluene. The reactor was flushed with synthesis gas (a 1 : 1 mixture of H_2 and CO gas) followed by charging to the desired pressure at room temperature. The reactor was heated to the desired temperature with a stirring speed of 340 rpm. After completion of the reaction, the reactor was cooled to room temperature in an ice-water bath and the remaining synthesis gas was carefully released in a well-ventilated fume hood. The reaction mixture was quantitatively analysed by gas chromatography.

Crystal structure determination of compounds **1**, **2**, **4–6**, **10–12**, **14**, **16–18**, and **21**

Single crystal X-ray diffraction data collections were performed at 100–150 K using a Bruker Smart APEX CCD diffractometer with a graphite monochromated Mo-K α radiation source for **1**, **2**, **4**, **6**, **10**, **16**, **18** and **21**, and a Bruker D8 VENTURE PHOTON 100 CMOS with a Cu-K α radiation source for **5**, **14** and **17**. A Rigaku Saturn 724 diffractometer with a graphite monochromated Mo-K α radiation source was used for the data collection of complexes **11** and **12**. Full spheres of data were collected using a combination of three sets of 400 frames (0.5° width in ω) at $\varphi = 0$, 90, and 180° plus two sets of 800 frames (0.45° width in ω) at $\varphi = -30$, and 210° under the control of the APEX2⁴⁰ program suite. The raw data were reduced to F^2 values using SAINT⁴¹ software, and global refinements of unit cell parameters using 4256–9958 reflections chosen from the full data sets were performed. Multiple measurements of equivalent reflections provided the basis for empirical absorption corrections as well as corrections for any crystal deterioration

during the data collection (SADABS).⁴² The structures were solved by direct methods, and refined by full-matrix least-squares procedures using the SHELXTL program package.^{43,44} Hydrogen atoms were placed in calculated positions and included as riding contributions with isotropic displacement parameters tied to those of the attached non-hydrogen atoms. In complex **11**, the disordered solvent molecule could not be identified or modeled to a known solvent, so it was SQUEEZED using PLATON.^R The results indicated 128 electrons, and a volume of 284 Å³. In **21**, both allyl groups and one tetrafluoroborate anion are disordered over two resolved orientations. The disorder was modelled by restraining the two components of each disordered group to have comparable geometries. Pertinent crystallographic data and other experimental details are summarized in Tables 5–7. Crystallographic data for the structures reported in this paper have been deposited with the Cambridge Crystallographic Data Centre as supplementary publication no. CCDC 1408417 (compound **1**), 1408420 (compound **2**), and 1511158 (compound **4**), 1511161 (compound **5**), 1511159 (compound **6**), 1511160 (compound **10**), 1517753 (compound **11**), 1517754 (compound **12**), 1511155 (compound **14**), 1511156 (compound **16**), 1511157 (compound **17**), 1511162 (compound **18**) and 1511163 (compound **21**).

Acknowledgements

We are grateful to the Science & Engineering Research Board, New Delhi, for financial support of this work through grant no. SB/S1/IC-08/2014. We also thank the Department of Chemistry, the Indian Institute of Technology Bombay, Mumbai, for instrumentation facilities as well as spectral and analytical data. J. T. Mague thanks the Louisiana Board of Regents for the purchase of the APEX CCD diffractometer, an NSF-MRI grant no. 1228232 for the purchase of the D8 VENTURE diffractometer and the Chemistry Department of Tulane University for providing X-ray laboratory facilities.

Notes and references

- (a) A. Bader and E. Lindner, *Coord. Chem. Rev.*, 1991, **108**, 27–110; (b) M. S. Balakrishna, V. S. Reddy, S. S. Krishnamurthy, J. F. Nixon and J. C. T. R. B. St. Laurent, *Coord. Chem. Rev.*, 1994, **129**, 1–90; (c) P. Espinet and K. Soulantica, *Coord. Chem. Rev.*, 1999, **193–195**, 499–556; (d) J. R. Dilworth and N. Wheatley, *Coord. Chem. Rev.*, 1999, **200**, 89–158; (e) A. Grabulosa, J. Granell and G. Muller, *Coord. Chem. Rev.*, 2007, **251**, 25–90; (f) Z. Freixa and P. W. N. M. van Leeuwen, *Coord. Chem. Rev.*, 2008, **252**, 1775–1786; (g) S. H. Chikkali, J. I. van der Vlugt and J. N. H. Reek, *Coord. Chem. Rev.*, 2014, **262**, 1–15; (h) C. A. Bessel, P. Aggarwal, A. C. Marschilok and K. J. Takeuch, *Chem. Rev.*, 2001, **101**, 1031–1066; (i) W. Tang and X. Zhang, *Chem. Rev.*, 2003, **103**, 3029–3069; (j) P. Braunstein, *Chem. Rev.*, 2006, **106**, 134–159;

- (k) H. Fernandez-Perez, P. Etayo, A. Panossian and A. Vidal-Ferran, *Chem. Rev.*, 2011, **111**, 2119–2176; (l) J. Wu and A. S. C. Chan, *Acc. Chem. Res.*, 2006, **39**, 711–720; (m) J.-L. Xie and K.-L. Zhou, *Acc. Chem. Res.*, 2008, **41**, 581–593.
- 2 P. W. N. M. van Leeuwen, P. C. J. Kamer, J. N. H. Reek and P. Dierkes, *Chem. Rev.*, 2000, **100**, 2741–2769.
- 3 (a) A. Miyashita, A. Yasuda, H. Takaya, K. Toriumi, T. Ito, T. Souchi and R. Noyori, *J. Am. Chem. Soc.*, 1980, **102**, 7932–7934; (b) A. Miyashita, H. Takaya, T. Souchi and R. Noyori, *Tetrahedron*, 1984, **40**, 1245–1253; (c) M. Kranenburg, Y. E. M. van der Burgt, P. C. J. Kamer, P. W. N. M. van Leeuwen, K. Goubitz and J. Fraanje, *Organometallics*, 1995, **14**, 3081–3089; (d) M. Kranenburg, P. C. J. Kamer and P. W. N. M. van Leeuwen, *Eur. J. Inorg. Chem.*, 1998, 25–27; (e) J. F. Hartwig, *Acc. Chem. Res.*, 1998, **31**, 852–860; (f) J. P. Wolfe, S. Wagaw, J.-F. Marcoux and S. L. Buchwald, *Acc. Chem. Res.*, 1998, **31**, 805–818; (g) M. Ogasawara, K. Yoshida and T. Hayashi, *Organometallics*, 2000, **19**, 1567–1571.
- 4 (a) A. Bader and E. Lindner, *Coord. Chem. Rev.*, 1991, **108**, 27–110; (b) P. Braunstein and F. Naud, *Angew. Chem., Int. Ed.*, 2001, **40**, 680–699; (c) C. S. Slone, D. A. Weinberger and C. A. Mirkin, *Prog. Inorg. Chem.*, 2007, **48**, 233–350; (d) R. Lindner, B. van den Bosch, M. Lutz, J. N. H. Reek and J. I. van der Vlugt, *Organometallics*, 2011, **30**, 499–510; (e) S. Kumar, G. Mani, S. Mondal and P. K. Chattaraj, *Inorg. Chem.*, 2012, **51**, 12527–12539; (f) S. Y. de Boer, Y. Gloaguen, J. N. H. Reek, M. Lutz and J. I. van der Vlugt, *Dalton Trans.*, 2012, **41**, 11276–11283; (g) W.-C. Lee, J. M. Sears, R. A. Enow, K. Eads, D. A. Krogstad and B. J. Frost, *Inorg. Chem.*, 2013, **52**, 1737–1746; (h) N. D. Jones, S. J. L. Foo, B. O. Patrick and B. R. James, *Inorg. Chem.*, 2004, **43**, 4056–4063; (i) J. A. Casares, P. Espinet, J. M. Martin-Alvarez and V. Santos, *Inorg. Chem.*, 2006, **45**, 6628–6636; (j) J. Zhang, R. Pattacini and P. Braunstein, *Inorg. Chem.*, 2009, **48**, 11954–11962; (k) L. J. Hounjet, R. McDonald, M. J. Ferguson and M. Cowie, *Inorg. Chem.*, 2011, **50**, 5361–5378; (l) N. Tsukada, T. Tamura and Y. Inoue, *Organometallics*, 2002, **21**, 2521–2528; (m) Y. Yamaguchi, K. Yamanishi, M. Kondo and N. Tsukada, *Organometallics*, 2013, **32**, 4837–4842.
- 5 (a) D. M. Zink, T. Baumann, M. Nieger, E. C. Barnes, W. Klopper and S. Bräse, *Organometallics*, 2011, **30**, 3275–3283; (b) D. M. Zink, T. Baumann, J. Friedrichs, M. Nieger and S. Bräse, *Inorg. Chem.*, 2013, **52**, 13509–13520; (c) D. M. Zink, M. Bächle, T. Baumann, M. Nieger, M. Kühn, C. Wang, W. Klopper, U. Monkowius, T. Hofbeck, H. Yersin and S. Bräse, *Inorg. Chem.*, 2013, **52**, 2292–2305.
- 6 (a) G. Erdogan and D. B. Grotjahn, *J. Am. Chem. Soc.*, 2009, **131**, 10354–10355; (b) D. B. Grotjahn, *Dalton Trans.*, 2008, 6497–6508; (c) S. Harkal, F. Rataboul, A. Zapf, C. Fuhrmann, T. Riermeier, A. Monsees and M. Beller, *Adv. Synth. Catal.*, 2004, **346**, 1742–1748; (d) C. Tejel, R. Bravi, M. A. Ciriano, L. A. Oro, M. Bordonaba, C. Graiff, A. Tiripicchio and A. Burini, *Organometallics*, 2000, **19**, 3115–3119.
- 7 (a) A. Burini, B. R. Pietroni, R. Galassi, G. Valle and S. Calogero, *Inorg. Chim. Acta*, 1995, **229**, 299–305; (b) M. Abdul Jalil, T. Yamada, S. Fujinami, T. Honjo and H. Nishikawa, *Polyhedron*, 2001, **20**, 627–633; (c) C. Tejel, M. A. Ciriano, R. Bravi, L. A. Oro, C. Graiff, R. Galassi and A. Burini, *Inorg. Chim. Acta*, 2003, **347**, 129–136; (d) V. J. Catalano and S. J. Horner, *Inorg. Chem.*, 2003, **42**, 8430–8438; (e) A. Caballero, F. A. Jalon, B. R. Manzano, G. Espino, M. Perez-Manrique, A. Mucientes, F. J. Poblete and M. Maestro, *Organometallics*, 2004, **23**, 5694–5706; (f) B. Milde, R. Packheiser, S. Hildebrandt, D. Schaarschmidt, T. Ruffer and H. Lang, *Organometallics*, 2012, **31**, 3661–3671.
- 8 (a) A. Antinolo, F. Carrillo-Hermosilla, E. Diez-Barra, J. Fernandez-Baeza, M. Fernandez-Lopez, A. Lara-Sanchez, A. Moreno, A. Otero, A. Maria Rodriguez and J. Tejada, *J. Chem. Soc., Dalton Trans.*, 1998, 3737–3744; (b) A. Otero, F. Carrillo-Hermosilla, P. Terreros, T. Exposito, S. Rojas, J. Fernandez-Baeza, A. Antinolo and I. J. Lopez-Solera, *Eur. J. Inorg. Chem.*, 2003, **2003**, 3233–3241; (c) S. A. Bhat, J. T. Mague and M. S. Balakrishna, *Dalton Trans.*, 2015, **44**, 17696–17703.
- 9 (a) Y. Canac, N. Debono, L. Vendier and R. Chauvin, *Inorg. Chem.*, 2009, **48**, 5562–5568; (b) C. Barthes, C. Lepetit, Y. Canac, C. Duhayon, D. Zargarian and R. Chauvin, *Inorg. Chem.*, 2012, **52**, 48–58; (c) Y. Canac, N. Debono, C. Lepetit, C. Duhayon and R. Chauvin, *Inorg. Chem.*, 2011, **50**, 10810–10819; (d) I. O. Koshevoy, L. Koskinen, E. S. Smirnova, M. Haukka, T. A. Pakkanen, A. S. Melnikov and S. P. Tunik, *Z. Anorg. Allg. Chem.*, 2010, **636**, 795–802.
- 10 (a) G. S. Ananthnag, J. T. Mague and M. S. Balakrishna, *Inorg. Chem.*, 2015, **54**, 10985–10992; (b) M. M. Siddiqui, J. T. Mague and M. S. Balakrishna, *Inorg. Chem.*, 2015, **54**, 6063–6065; (c) M. M. Siddiqui, J. T. Mague and M. S. Balakrishna, *Inorg. Chem.*, 2015, **54**, 1200–1202; (d) S. Naik, M. Kumaravel, J. T. Mague and M. S. Balakrishna, *Inorg. Chem.*, 2014, **53**, 1370–1381; (e) B. Punji, J. T. Mague and M. S. Balakrishna, *Inorg. Chem.*, 2007, **46**, 11316–11327; (f) R. Venkateswaran, J. T. Mague and M. S. Balakrishna, *Inorg. Chem.*, 2007, **46**, 809–817.
- 11 (a) D. W. Allen and B. F. Taylor, *J. Chem. Soc., Dalton Trans.*, 1982, 51–54; (b) M. N. Chevykalova, L. F. Manzhukova, N. V. Artemova, Yu. N. Luzikov, I. E. Nifantev and E. E. Nifantev, *Russ. Chem. Bull. Int. Ed.*, 2003, **52**, 78–84.
- 12 (a) A. P. Alba, H. de la Riva, H. Nieuwhuyzen, D. Bautista, P. R. Raithby, H. A. Sparkes, S. J. Teat, J. M. Lopez-de Luzuriaga and M. C. Lagunas, *Dalton Trans.*, 2004, 3459–3467; (b) M. F. Cain, S. C. Reynolds, B. J. Anderson, D. S. Glueck, J. A. Golen, C. E. Moore and A. L. Rheingold, *Inorg. Chim. Acta*, 2011, **369**, 55–61.
- 13 (a) S. Sauerbrey, P. K. Majhi, J. Daniels, G. Schnakenburg, G. M. Brändle, K. Scherer and R. Streubel, *Inorg. Chem.*, 2011, **50**, 793–799; (b) B. Milde, D. Schaarschmidt, T. Ruffer and H. Lang, *Dalton Trans.*, 2012, **41**, 5377–5390; (c) P. W. Coddling and K. A. Kerr, *Acta Crystallogr., Sect. B:*

- Struct. Crystallogr. Cryst. Chem.*, 1979, **35**, 1261–1263; (d) B. Milde, M. Lohan, C. Schreiner, T. Ruffer and H. Lang, *Eur. J. Inorg. Chem.*, 2011, 5437–5449.
- 14 (a) S. A. Bhat, J. T. Mague and M. S. Balakrishna, *Inorg. Chim. Acta*, 2016, **443**, 243–250; (b) S. A. Bhat, J. T. Mague and M. S. Balakrishna, *Polyhedron*, 2016, **107**, 190–195.
- 15 (a) J. Cai, X. Yang, K. Arumugam, C. W. Bielawski and J. L. Sessler, *Organometallics*, 2011, **30**, 5033–5037; (b) B. Chaubey, S. M. Mobin and M. S. Balakrishna, *Dalton Trans.*, 2014, **43**, 584–591.
- 16 P. C. Kunz, I. Thiel, A. L. Noffke, G. J. Reiß, F. Mohr and B. Spingler, *J. Organomet. Chem.*, 2012, **697**, 33–40.
- 17 A. Brink, A. Roodt, G. Steyl and H. G. Visser, *Dalton Trans.*, 2010, **39**, 5572–5578.
- 18 M. J. Bennett and P. B. Donaldson, *Inorg. Chem.*, 1977, **16**, 655–660.
- 19 J. Albers, E. Dinjus, S. Pitter and O. Walter, *J. Mol. Catal.*, 2004, **219**, 41–46.
- 20 G. Esquiús, J. Pons, R. Yáñez, J. Ros, R. Mathieu, B. Donnadiu and N. Lugan, *Eur. J. Inorg. Chem.*, 2002, 2999–3006.
- 21 S. Burling, L. D. Field, B. A. Messerle, K. Q. Vuong and P. Turner, *Dalton Trans.*, 2003, 4181–4191.
- 22 P. E. Garrou, *Chem. Rev.*, 1981, **81**, 229–266.
- 23 C. J. Cobley and P. G. Pringle, *Inorg. Chim. Acta*, 1997, **265**, 107–115.
- 24 E. Lindner, R. Fawzi, H. A. Mayer, K. Eichele and W. Hiller, *Organometallics*, 1992, **11**, 1033–1043.
- 25 T. Hayashi, M. Konishi, Y. Kobori, M. Kumada, T. Higuchi and K. Hirotsu, *J. Am. Chem. Soc.*, 1984, **106**, 158–163.
- 26 M. A. Zuideveld, B. H. G. Swennenhuis, M. D. K. Boele, Y. Guari, G. P. F. van Strijdonck, J. N. H. Reek, P. C. J. Kamer, K. Goubitz, J. Fraanje, M. Lutz, A. L. Spek and P. W. N. M. van Leeuwen, *J. Chem. Soc., Dalton Trans.*, 2002, 2308–2317.
- 27 W. L. Steffen and G. J. Palenik, *Inorg. Chem.*, 1976, **15**, 2432–2439.
- 28 K. Saikia, B. Deb, B. J. Borah, P. P. Sarmah and D. K. Dutta, *J. Organomet. Chem.*, 2012, **696**, 4293–4297.
- 29 R. J. van Haaren, K. Goubitz, J. Fraanje, G. P. F. van Strijdonck, H. Oevering, B. Coussens, J. N. H. Reek, P. C. J. Kamer and P. W. N. M. van Leeuwen, *Inorg. Chem.*, 2001, **40**, 3363–3372.
- 30 P. W. N. M. van Leeuwen and C. Claver, *Rhodium Catalyzed Hydroformylation*, Kluwer Academic Publishers, Dordrecht, 2000.
- 31 H. You, Y. Wang, X. Zhao, S. Chen and Y. Liu, *Organometallics*, 2013, **32**, 2698–2704.
- 32 S.-J. Chen, Y.-Q. Li, Y.-Y. Wang, X.-L. Zhao and Y. Liu, *J. Mol. Catal.*, 2015, **396**, 68–76.
- 33 S.-J. Chen, Y.-Y. Wang, Y.-Q. Li, X.-L. Zhao and Y. Liu, *Catal. Commun.*, 2014, **50**, 5–8.
- 34 E. Diez-Barra, A. De Hoz, R. I. Rodriguez-Curiel and J. Tejada, *Tetrahedron*, 1997, **53**, 2253–2260.
- 35 M. A. Bennett, T. N. Huang, T. W. Matheson and A. K. Smith, *Inorg. Synth.*, 1982, **21**, 74–78.
- 36 G. Giordano and R. H. Crabtree, *Inorg. Synth.*, 1990, **28**, 88–90.
- 37 R. Cramer, J. A. McCleverty and J. Bray, *Inorg. Synth.*, 1990, **28**, 86–88.
- 38 D. Drew and J. R. Doyle, *Inorg. Synth.*, 1990, **28**, 346–349.
- 39 Y. Tatsuno, T. Yoshida and S. Otsuka, *Inorg. Synth.*, 1990, **28**, 342–343.
- 40 APEX2, Bruker-AXS, Madison, WI, 2013.
- 41 SAINT, Bruker-AXS, Madison, WI, 2010.
- 42 G. M. Sheldrick, SADABS, University of Gottingen, Germany, 2008.
- 43 G. M. Sheldrick, *Acta Crystallogr., Sect. A: Fundam. Crystallogr.*, 2008, **64**, 112–122.
- 44 SHELXTL, Version 2008/4, Bruker-AXS, Madison, WI, 2008.